

Hopf Bifurcation Control of a Fractional-Order Delayed Turbidostat Model via a Novel Extended Hybrid Controller

Changjin Xu^{a,*}, Wei Ou^b, Yicheng Pang^b, Qingyi Cui^b,
Mati ur Rahman^c, Muhammad Farman^d, Shabir
Ahmad^e, Anwar Zeb^f

^a *Guizhou Key Laboratory of Economics System Simulation, Guizhou
University of Finance and Economics, Guiyang 550025, PR China*

^b *School of Mathematics and Statistics, Guizhou University of Finance
and Economics, Guiyang 550025, PR China*

^c *School of Mathematical Science, Shanghai Jiao Tong University,
Shanghai 200240, PR China*

^d *Department of Mathematics, Khawaja Fareed University of Engineering
and Information Technology, Rahim Yar Khan, Pakistan*

^e *Department of Mathematics, University of Malakand, Chakdara, Dir
Lower, Khyber Pakhtunkhwa, Pakistan*

^f *Department of Mathematics, COMSATS University Islamabad,
Abbottabad Campus, Abbottabad, 22060, Khyber, Pakhtunkhwa, Pakistan*

xcj403@126.com, ouyiyich@163.com, ypanggy@outlook.com,

cqy5388427@163.com, mati-maths_374@sjtu.edu.cn,

farmanlink@gmail.com, shabirahmad2232@gmail.com, anwar@cuiatd.edu.pk

(Received August 8, 2023)

Abstract

Building delayed dynamical models to describe the inherent laws
of different chemical matters has become a hot theme in recent years.

*Corresponding author.

In this current study, we set up a new fractional-order delayed turbidostat model. By using Laplace transform, we obtain the characteristic equation of established fractional-order delayed turbidostat model. By selecting the delay as bifurcation parameter and exploring the roots of the corresponding characteristic equation of the involved fractional-order delayed turbidostat model, a novel delay-dependent condition on stability and Hopf bifurcation is acquired. Taking advantage of a novel extended hybrid controller, the stability region and the time of Hopf bifurcation of the established fractional-order delayed turbidostat model are successfully controlled. The role of delay in stabilizing system and controlling Hopf bifurcation is revealed. Matlab experiments are carried out to check the rationality of the acquired key outcomes in this article. The acquired outcomes of this study are completely new and own great theoretical value in dominating concentrations of various chemical matters.

1 Introduction

During the past decades, delayed dynamical equation has witnessed great application in many natural science and social science. In particular, setting up some suitable delayed dynamical equations to reveal the intrinsic chemical reaction law has become a hotspot issue in chemistry. By investigating the dynamical behavior of the formulated delayed differential chemical reaction models, we can effectively grasp the variation law among different chemical substances and then better serve humanity. In recent years, a number of researchers are dedicated to exploring various dynamics of all kinds of chemical reaction models and a great deal of worthwhile results on chemical reaction models have been achieved. For instance, Xu and Wu [1] dealt with Hopf bifurcation and the control issue of chaos of a chemical reaction system; Wang and Jia [2] investigated the stability and bifurcation in a Gray-Scott chemical reaction system; Zhang and He [3] discussed the multiple stability switches and bifurcation driven by time delay for a Lengyel-Epstein chemical reaction model; Eskandari et al. [4] explored the Neimark-Sacker bifurcation of a discrete-time chemical reaction system; In 2018, Din et al. [5] carried out the stability, Neimark-Sacker bifurcation and chaos control analysis on chlorine dioxide-iodine-malonic acid reaction model. In details, one can see [6–11].

We know that chemostat is an important laboratory instrument utilized for the continuous culture of microorganisms [12]. It plays a vital role in population dynamics and microbiology. The chemostat can be regarded as the simplest idealization of biological model and it has measurable parameters, reasonable experiments and tractable trait in mathematics [12, 13]. During the past decades, many scholars pay great attention to the various chemostat models to maintain the coexistence of the organisms(see [12–15]). Turbidostat is a special chemostat owning feedback control of the dilution rate [16, 17]. The optical sensor in turbidostat can effectively measure the turbidity of the fluid and this signal can be applied to adjust the rate of dilution. Flegr [18], De Leenheer and Smith [19] dealt with the coexistence issue of both species in turbidostat. The turbidostat model takes the following form:

$$\begin{cases} \frac{dw_1(t)}{dt} = A(w)(w_0 - w_1) - \frac{w_2}{\gamma_1}g_1(w_1) - \frac{w_3}{\gamma_2}g_2(w_1), \\ \frac{dw_2(t)}{dt} = w_2[g_1(w_1) - A(w)], \\ \frac{dw_3(t)}{dt} = w_3[g_2(w_1) - A(w)], \end{cases} \quad (1)$$

where $w_1(t)$ stands for the limiting nutrient concentration and $w_2(t)$ stands for the concentration of the first competitor at time t and $w_3(t)$ stands for the concentration of the second competitor at time t ; w_0 represents the input concentration of the limiting nutrient; $\gamma_j(j = 1, 2)$ denote yield constants. g_i is called uptakes function and is a continuously differentiable function and $g_i(0) = 0$ and $g'_i(w_1) > 0$ for arbitrary $w_1 \in R_+$. In general, g_i takes the following form:

$$g_i(w_1) = \frac{w_j}{\alpha_j + w_1}, j = 1, 2, \quad (2)$$

where $\alpha_j, w_j(j = 1, 2)$ stand for the halfsaturation constant of the j th competitor(or Michaelis-Menten constant) and the maximal growth rate, respectively; $A(w)$ denotes the dilution of the turbidostat and takes the following form:

$$A(w) = a + \kappa_1 w_2(t) + \kappa_2 w_3(t), \quad (3)$$

where $\kappa_1, \kappa_2, a > 0$. In details, one can consult [18, 19]. In practice, although the sensor is very sensitive, there usually exists delay during the process of measurement for fluid turbidity. The delayed signal has a vital effect on controlling the dilution rate. Stimulated by this viewpoint, Yuan et al. [12] set up the following delayed turbidostat model owning delayed feedback control:

$$\begin{cases} \frac{dw_1(t)}{dt} = [a + \kappa_1 w_2(t - \vartheta) + \kappa_2 w_3(t - \vartheta)](w_0 - w_1) \\ \quad - \frac{w_2}{\gamma_1} g_1(w_1) - \frac{w_3}{\gamma_2} g_2(w_1), \\ \frac{dw_2(t)}{dt} = w_2 [g_1(w_1) - (a + \kappa_1 w_2(t - \vartheta) + \kappa_2 w_3(t - \vartheta))], \\ \frac{dw_3(t)}{dt} = w_3 [g_2(w_1) - (a + \kappa_1 w_2(t - \vartheta) + \kappa_2 w_3(t - \vartheta))], \end{cases} \quad (4)$$

where ϑ is a delay, which stands for feedback time. By selecting the delay as bifurcation parameter, Yuan et al. [12] studied the stability and the existence of Hopf bifurcation of model (1.4). In addition, the bifurcation peculiarities of model (1.4) have been explored via center manifold theory and normal form theorem.

It should be noted that all the involved publications above on turbidostat models (see [1–19]) are merely concerned with the integer-order turbidostat models. For a long time, fractional-order differential equation has maintained a relatively slow development state due to the lack of basic theoretical tools and practical application background. In recent years, a lot of research shows that fractional-order differential equation is a vital theoretical tool in describing the true laws of nature since it owns the strong memory peculiarity and advantage of hereditary for different substances and development processes [20–23]. Recently, fractional differential equation has been extensively used in many area such as financial engineering, complex networks, cryptology, multifarious waves in physics, aeroelasticity, capacitor principle, bioengineering, automation and so on [24–27]. At present, great accomplishments on fractional dynamical systems have been acquired. For example, Rihan and Rajivganthi [28] studied the Hopf bifurcation and stability of a fractional-order delay predator-prey model involving Holling-type III function; Wang et al. [29] investigated the bifur-

cation phenomenon and stability for a fractional-order delayed predator-prey model owning interspecific competition; Xiao et al. [30] discussed controller design of finite-time synchronization in fractional memristive neural network models; Liu et al. [31] explored the event-triggered bipartite synchronization issue of coupled fractional-order neural networks. For more concrete contents, one can see [32–45].

Considering that the delayed turbidostat model owning delayed feedback control can better describe the memory peculiarity and advantage of hereditary for the concentrations of three chemical reactants and inspired by the exploration above and depending on system (4), in this study, we will set up the following fractional-order delayed turbidostat model owning delayed feedback control:

$$\left\{ \begin{array}{l} \frac{d^p w_1(t)}{dt^p} = [a + \kappa_1 w_2(t - \vartheta) + \kappa_2 w_3(t - \vartheta)](w_0 - w_1) \\ \quad - \frac{w_2}{\gamma_1} g_1(w_1) - \frac{w_3}{\gamma_2} g_2(w_1), \\ \frac{d^p w_2(t)}{dt^p} = w_2 [g_1(w_1) - (a + \kappa_1 w_2(t - \vartheta) + \kappa_2 w_3(t - \vartheta))], \\ \frac{d^p w_3(t)}{dt^p} = w_3 [g_2(w_1) - (a + \kappa_1 w_2(t - \vartheta) + \kappa_2 w_3(t - \vartheta))], \end{array} \right. \quad (5)$$

where $p \in (0, 1]$. All other parameters own the identical connotation as those in system (4).

In this study, we will explore the following two aspects: **(a)** Investigate the stability behavior and the generation of Hopf bifurcation of model (5). **(b)** Adjust the stability region and the time of appearance of Hopf bifurcation of model (5) via extended hybrid controller.

The elementary structure of this study is organized as follows. Some rudimentary principles about fractional-order differential equation are provided in Segment 2. Segment 3 handles the stability behavior and the existence of Hopf bifurcation of model (5) and a new delay-independent stability and bifurcation condition of model (5) is acquired. Segment 4 deals with the control problem of stability region and the time of onset of Hopf bifurcation for model (5) via a novel extended hybrid controller. Segment 5 carries out computer experiments to validate the validity of the gained key conclusions. Segment 6 ends this study with a succinct

conclusion.

2 Rudimentary knowledge

In this segment, some essential basic theories about fractional-order differential equation are presented.

Definition 2.1. [46] *The fractional integral of order p of the function $\omega(\mu)$ is given by*

$$\mathcal{I}^p \omega(\mu) = \frac{1}{\Gamma(p)} \int_{\mu_0}^{\mu} (\mu - u)^{p-1} \omega(u) du,$$

where $\mu > \mu_0, p > 0, \Gamma(u) = \int_0^{\infty} s^{u-1} e^{-s} ds$ denotes the Gamma function.

Definition 2.2. [47] *Define the Caputo fractional-order derivative of order p of the function $\omega(\mu) \in ([\mu_0, \infty), R)$ as follows:*

$$\mathcal{D}^p \omega(\mu) = \frac{1}{\Gamma(m-p)} \int_{\mu_0}^{\mu} \frac{\omega^{(n)}(s)}{(\mu-s)^{p-n+1}} ds,$$

where $\mu \geq \mu_0$ and n stands for a positive integer ($n-1 \leq p < n$). Particularly, if $p \in (0, 1)$, then

$$\mathcal{D}^p \omega(\mu) = \frac{1}{\Gamma(1-p)} \int_{\mu_0}^{\mu} \frac{\omega'(s)}{(\mu-s)^p} ds.$$

Lemma 2.1. [48] *Consider the system: $\mathcal{D}^p v = \mathcal{H}v, v(0) = v_0$ where $p \in (0, 1), v \in R^n, \mathcal{H} \in R^{n \times n}$. Assume that $\chi_l (l = 1, 2, \dots, n)$ is the root of the characteristic equation of $\mathcal{D}^p v = \mathcal{H}v$, then system $\mathcal{D}^p v = \mathcal{H}v$ is locally asymptotically stable $\Leftrightarrow |\arg(\chi_l)| > \frac{p\pi}{2} (l = 1, 2, \dots, n)$. The system is stable $\Leftrightarrow |\arg(\chi_l)| > \frac{p\pi}{2} (l = 1, 2, \dots, n)$ and every critical eigenvalue satisfying $|\arg(\chi_l)| = \frac{p\pi}{2} (l = 1, 2, \dots, n)$ owns geometric multiplicity one.*

3 Bifurcation investigation

According to the work of Yuan et al. [12], we know that if the following condition holds,

$$(Q_1) \text{ (i) } a \in (0, A^*), \text{ (ii) } \kappa_1 < \frac{A^* - a}{1 - w_1^*} < \kappa_2 \text{ or } \kappa_2 < \frac{A^* - a}{1 - w_1^*} < \kappa_1$$

where A^* satisfies $g_1(w_1^*) = g_2(w_1^*) = A^*$, where $A^* \in (0, 1)$, $g_1'(w_1^*) \neq g_2'(w_1^*)$, then system (5) admits a unique positive equilibrium point $W(w_{1*}, w_{2*}, w_{3*})$, where

$$\begin{cases} w_{2*} = \frac{A^* - \kappa_2(1 - w_{1*}) - a}{\kappa_1 - \kappa_2}, \\ w_{3*} = \frac{\kappa_1(1 - w_{1*}) - A^* + a}{\kappa_1 - \kappa_2}. \end{cases} \quad (6)$$

The linear system of system (5) at $W(w_{1*}, w_{2*}, w_{3*})$ owns the following form:

$$\mathcal{D}^p w(t) = A_1 w(t) + A_2 w(t - \theta), \quad (7)$$

where

$$\begin{cases} w(t) = \begin{bmatrix} w_1(t) \\ w_2(t) \\ w_3(t) \end{bmatrix}, \\ A_1 = \begin{bmatrix} a_1 & a_2 & a_3 \\ a_4 & 0 & 0 \\ a_5 & 0 & 0 \end{bmatrix}, \\ A_2 = \begin{bmatrix} 0 & b_1 & b_2 \\ 0 & b_3 & b_4 \\ 0 & b_5 & b_6 \end{bmatrix}, \end{cases} \quad (8)$$

where

$$\left\{ \begin{array}{l} a_1 = - \left[a + \kappa_1 w_{2*} + \kappa_3 w_{3*} + \frac{g'_1(w_{1*})}{\gamma_1} + \frac{g'_2(w_{1*})}{\gamma_2} \right], \\ a_2 = - \frac{g_1(w_{1*}) + g'_1(w_{1*})}{\gamma_1}, \\ a_3 = - \frac{g_2(w_{1*}) + g'_2(w_{1*})}{\gamma_2}, \\ a_4 = w_{2*} g'_1(w_{1*}), \\ a_5 = w_{3*} g'_2(w_{1*}), \\ b_1 = \kappa_1 (w_0 - w_{1*}), \\ b_2 = \kappa_2 (w_0 - w_{1*}), \\ b_3 = -\kappa_1 w_{2*}, \\ b_4 = -\kappa_2 w_{2*}, \\ b_5 = -\kappa_1 w_{3*}, \\ b_6 = -\kappa_2 w_{3*}. \end{array} \right. \quad (9)$$

The characteristic equation of system (7) reads as

$$\det \begin{bmatrix} s^p - a_1 & -a_2 - b_1 e^{-s\vartheta} & -a_3 - b_2 e^{-s\vartheta} \\ -a_4 & s^p - b_3 e^{-s\vartheta} & -b_4 e^{-s\vartheta} \\ -a_5 & -b_5 e^{-s\vartheta} & s^p - b_6 e^{-s\vartheta} \end{bmatrix} = 0, \quad (10)$$

which results in

$$s^{3p} + b_1 s^{2p} + b_2 s^p + b_3 + (b_4 s^p + b_5) e^{-s\vartheta} + (b_6 s^p + b_7) e^{-2s\vartheta} = 0, \quad (11)$$

where

$$\left\{ \begin{array}{l} b_1 = -a_1, \\ b_2 = -(a_2 a_4 + a_3 a_5), \\ b_3 = a_1 b_4 b_5, \\ b_4 = a_1 b_3 + a_1 b_6 - a_5 b_2 - a_4 b_1, \\ b_5 = a_3 a_5 b_3 + a_2 a_4 a_6 b_6 - a_2 a_5 b_2 - a_3 a_4 b_5, \\ b_6 = b_3 b_6 - b_4 b_5, \\ b_7 = a_1 b_3 b_6 - a_5 b_1 b_4 - a_4 b_2 b_5 + a_5 b_2 b_3 + a_4 b_1 b_6. \end{array} \right. \quad (12)$$

When $\theta = 0$, then Eq.(11) has the following form:

$$\lambda^3 + b_1\lambda^2 + (b_2 + b_4 + b_6)\lambda + b_3 + b_5 + b_7 = 0. \quad (13)$$

If

$$(Q_2) \begin{cases} \Delta_1 = b_1 > 0, \\ \Delta_2 = \det \begin{bmatrix} b_1 & 1 \\ b_3 + b_5 + b_7 & b_2 + b_4 + b_6 \end{bmatrix}, \\ \Delta_3 = (b_3 + b_5 + b_7)\Delta_2 > 0 \end{cases},$$

is fulfilled, then the three roots $\lambda_1, \lambda_2, \lambda_3$ of Eq. (13) obey $|\arg(\lambda_1)| > \frac{p\pi}{2}, |\arg(\lambda_2)| > \frac{p\pi}{2}, |\arg(\lambda_3)| > \frac{p\pi}{2}$. In view of Lemma 2.1, we can understand that the positive equilibrium point $W(w_{1*}, w_{2*}, w_{3*})$ of system (5) with the delay $\vartheta = 0$ maintains locally asymptotically stability.

By (11), we have

$$(s^{3p} + b_1s^{2p} + b_2s^p + b_3)e^{s\vartheta} + (b_4s^p + b_5) + (b_6s^p + b_7)e^{-s\vartheta} = 0. \quad (14)$$

Suppose that $s = i\varepsilon = \varepsilon \left(\cos \frac{\pi}{2} + i \sin \frac{\pi}{2} \right)$ is the root of Eq. (14). Then by Eq.(14), one gains

$$\begin{aligned} & \left[\varepsilon^{3p} \left(\cos \frac{3p\pi}{2} + i \sin \frac{3p\pi}{2} \right) + b_1\varepsilon^{2p}(\cos p\pi + i \sin p\pi) \right. \\ & \left. + b_2\varepsilon^p \left(\cos \frac{p\pi}{2} + i \sin \frac{p\pi}{2} \right) + b_3 \right] (\cos \varepsilon\vartheta + i \sin \varepsilon\vartheta) \\ & + \left[b_4\varepsilon^p \left(\cos \frac{p\pi}{2} + i \sin \frac{p\pi}{2} \right) + b_5 \right] + \left[b_6\varepsilon^p \left(\cos \frac{p\pi}{2} + i \sin \frac{p\pi}{2} \right) + b_7 \right] \\ & \times (\cos \varepsilon\vartheta - i \sin \varepsilon\vartheta) = 0. \end{aligned} \quad (15)$$

Then it follows from (15) that

$$\begin{cases} \Phi_1(\varepsilon) \cos \varepsilon\vartheta - \Phi_2(\varepsilon) \sin \varepsilon\vartheta = -\Phi_3(\varepsilon), \\ \Phi_4(\varepsilon) \cos \varepsilon\vartheta + \Phi_5(\varepsilon) \sin \varepsilon\vartheta = -\Phi_6(\varepsilon), \end{cases} \quad (16)$$

where

$$\left\{ \begin{array}{l} \Phi_1(\varepsilon) = c_1\varepsilon^{3p} + c_2\varepsilon^{2p} + c_3\varepsilon^p + c_4, \\ \Phi_2(\varepsilon) = c_5\varepsilon^{3p} + c_6\varepsilon^{2p} + c_7\varepsilon^p, \\ \Phi_3(\varepsilon) = c_8\varepsilon^p + c_9, \\ \Phi_4(\varepsilon) = c_{10}\varepsilon^{3p} + c_{11}\varepsilon^{2p} + c_{12}\varepsilon^p, \\ \Phi_5(\varepsilon) = c_{13}\varepsilon^{3p} + c_{14}\varepsilon^{2p} + c_{15}\varepsilon^p + c_{16}, \\ \Phi_6(\varepsilon) = c_{17}\varepsilon^p, \end{array} \right. \quad (17)$$

where

$$\left\{ \begin{array}{l} c_1 = \cos \frac{3p\pi}{2}, \\ c_2 = b_1 \cos p\pi, \\ c_3 = (b_2 + b_6) \cos \frac{p\pi}{2}, \\ c_4 = b_3 + b_7, \\ c_5 = \sin \frac{3p\pi}{2}, \\ c_6 = b_1 \sin p\pi, \\ c_7 = (b_2 - b_6) \sin \frac{p\pi}{2}, \\ c_8 = b_4 \cos \frac{p\pi}{2}, \\ c_9 = b_5, \\ c_{10} = \sin \frac{3p\pi}{2}, \\ c_{11} = b_1 \sin p\pi, \\ c_{12} = (b_2 + b_6) \sin \frac{p\pi}{2}, \\ c_{13} = \cos \frac{3p\pi}{2}, \\ c_{14} = b_1 \cos p\pi, \\ c_{15} = (b_2 - b_6) \cos \frac{p\pi}{2}, \\ c_{16} = b_3 - b_7, \\ c_{17} = b_4 \sin \frac{p\pi}{2}. \end{array} \right. \quad (18)$$

By (3.11), we have

$$\left\{ \begin{array}{l} \cos \varepsilon\vartheta = -\frac{\Phi_3(\varepsilon)\Phi_5(\varepsilon) + \Phi_2(\varepsilon)\Phi_6(\varepsilon)}{\Phi_1(\varepsilon)\Phi_5(\varepsilon) + \Phi_2(\varepsilon)\Phi_4(\varepsilon)}, \\ \sin \varepsilon\vartheta = \frac{\Phi_1(\varepsilon)\Phi_6(\varepsilon) - \Phi_3(\varepsilon)\Phi_4(\varepsilon)}{\Phi_1(\varepsilon)\Phi_5(\varepsilon) + \Phi_2(\varepsilon)\Phi_4(\varepsilon)}. \end{array} \right. \quad (19)$$

In view of $\cos^2 \varepsilon\vartheta + \sin^2 \varepsilon\vartheta = 1$, it follows from (19) that

$$\begin{aligned} & [\Phi_3(\varepsilon)\Phi_5(\varepsilon) + \Phi_2(\varepsilon)\Phi_6(\varepsilon)]^2 + [\Phi_1(\varepsilon)\Phi_6(\varepsilon) - \Phi_3(\varepsilon)\Phi_4(\varepsilon)]^2 \\ &= [\Phi_1(\varepsilon)\Phi_5(\varepsilon) + \Phi_2(\varepsilon)\Phi_4(\varepsilon)]^2, \end{aligned} \quad (20)$$

which results in

$$\begin{aligned} & d_1\varepsilon^{12p} + d_2\varepsilon^{11p} + d_3\varepsilon^{10p} + d_4\varepsilon^{9p} + d_5\varepsilon^{8p} + d_6\varepsilon^{7p} + d_7\varepsilon^{6p} \\ &+ d_8\varepsilon^{5p} + d_9\varepsilon^{4p} + d_{10}\varepsilon^{3p} + d_{11}\varepsilon^{2p} + d_{12}\varepsilon^p + d_{13} = 0, \end{aligned} \quad (21)$$

where

$$\begin{aligned} d_1 &= (c_1c_{13} + c_5c_{10})^2, \\ d_2 &= 2(c_1c_{13} + c_5c_{10})(c_1c_{14} + c_2c_{13} + c_5c_{11} + c_6c_{10}) \\ d_3 &= (c_1c_{14} + c_2c_{13} + c_5c_{11} + c_6c_{10})^2 - 2(c_1c_{13} + c_5c_{10}) \\ &\quad \times (c_1c_{15} + c_2c_{14} + c_3c_{13} + c_5c_{12} + c_6c_{11} + c_7c_{10}), \\ d_4 &= 2(c_1c_{13} + c_5c_{10})(c_1c_{16} + c_2c_{15} + c_3c_{14} + c_6c_{12} + c_7c_{11}) \\ &\quad + 2(c_1c_{14} + c_2c_{13} + c_5c_{11} + c_6c_{10})(c_1c_{15} + c_2c_{14} + c_3c_{13} \\ &\quad + c_5c_{12} + c_6c_{11} + c_7c_{10}), \\ d_5 &= (c_1c_{15} + c_2c_{14} + c_3c_{13} + c_5c_{12} + c_6c_{11} + c_7c_{10})^2 \\ &\quad + 2(c_1c_{13} + c_5c_{10})(c_2c_{16} + c_3c_{15} + c_4c_{14} + c_7c_{12}) \\ &\quad + 2(c_1c_{14} + c_2c_{13} + c_5c_{11} + c_6c_{10})(c_1c_{16} + c_2c_{15} \\ &\quad + c_3c_{14} + c_4c_{13} + c_6c_{12} + c_7c_{11}) - (c_1c_{17} - c_8c_{10})^2 \\ &\quad - (c_8c_{13})^2, \\ d_6 &= 2(c_1c_{13} + c_5c_{10})(c_3c_{16} + c_4c_{15}) + 2(c_1c_{14} + c_2c_{13} \\ &\quad + c_5c_{11} + c_6c_{10})(c_2c_{16} + c_3c_{15} + c_4c_{14} + c_7c_{12}) \\ &\quad + 2(c_1c_{15} + c_2c_{14} + c_3c_{13} + c_5c_{12} + c_6c_{11} + c_7c_{10}) \\ &\quad \times (c_1c_{16} + c_2c_{15} + c_3c_{14} + c_4c_{13} + c_6c_{12} + c_7c_{11}) \\ &\quad - 2(c_1c_{17} - c_8c_{10})(c_2c_{17} - c_9c_{10} - c_8c_{11}) \\ &\quad - 2c_8c_{13}(c_9c_{13} + c_8c_{14} + c_6c_{17}), \end{aligned}$$

$$\begin{aligned}
d_7 = & (c_1c_{16} + c_2c_{15} + c_3c_{14} + c_4c_{13} + c_6c_{12} + c_7c_{11})^2 \\
& + 2c_4c_{16}(c_1c_{13} + c_5c_{10}) + 2(c_3c_{16} + c_4c_{15})(c_1c_{14} + c_2c_{13} \\
& + c_5c_{11} + c_6c_{10}) + 2(c_1c_{15} + c_2c_{14} + c_3c_{13} \\
& + c_5c_{12} + c_6c_{11} + c_7c_{10})(c_2c_{16} + c_3c_{15} + c_4c_{14} + c_7c_{12}) \\
& - (c_2c_{17} - c_9c_{10} - c_8c_{11})^2 - (c_9c_{13} + c_8c_{14} + c_6c_{17})^2 \\
& - 2c_8c_{13}(c_9c_{14} + c_8c_{15} + c_7c_{17}),
\end{aligned}$$

$$\begin{aligned}
d_8 = & 2c_4c_6(c_1c_{14} + c_2c_{13} + c_5c_{11} + c_6c_{10}) + 2(c_1c_{15} + c_2c_{14} \\
& + c_3c_{13} + c_5c_{12} + c_6c_{11} + c_7c_{10})(c_3c_{16} + c_4c_{15}) \\
& + 2(c_1c_{16} + c_2c_{15} + c_3c_{14} + c_4c_{13} + c_6c_{12} + c_7c_{11}) \\
& \times (c_2c_{16} + c_3c_{15} + c_4c_{14} + c_7c_{12}) - 2(c_1c_{17} \\
& - c_8c_{10})(c_4c_{17} - c_9c_{12}) - 2(c_2c_{17} - c_9c_{10} - c_8c_{11}) \\
& \times (c_3c_{17} - c_9c_{11} - c_8c_{12}) - 2c_8c_{13}(c_9c_{15} + c_8c_{16}) \\
& - 2(c_9c_{13} + c_8c_{14} + c_6c_{17})(c_9c_{14} + c_8c_{15} + c_7c_{17}),
\end{aligned}$$

$$\begin{aligned}
d_9 = & (c_2c_{16} + c_3c_{15} + c_4c_{14} + c_7c_{12})^2 + 2(c_3c_{16} + c_4c_{15}) \\
& \times (c_1c_{16} + c_2c_{15} + c_3c_{14} + c_4c_{13} + c_6c_{12} + c_7c_{11}) \\
& + 2c_4c_{16}(c_1c_{15} + c_2c_{14} + c_3c_{13} + c_5c_{12} + c_6c_{11} + c_7c_{10}) \\
& - (c_3c_{17} - c_9c_{11} - c_8c_{12})^2 - 2(c_2c_{17} - c_9c_{10} - c_8c_{11}) \\
& \times (c_4c_{17} - c_9c_{12}) - (c_9c_{14} + c_8c_{15} + c_7c_{17})^2 \\
& - 2(c_9c_{15} + c_8c_{16})(c_9c_{13} + c_8c_{14} + c_6c_{17}),
\end{aligned}$$

$$\begin{aligned}
d_{10} = & 2c_4c_{16}(c_1c_{16} + c_2c_{15} + c_3c_{14} + c_4c_{13} + c_6c_{12} + c_7c_{11}) \\
& + 2(c_3c_{16} + c_4c_{15})(c_2c_{16} + c_3c_{15} + c_4c_{14} + c_7c_{12}) \\
& - 2(c_3c_{17} - c_9c_{11} - c_8c_{12})(c_4c_{17} - c_9c_{12}) \\
& - 2c_9c_{16}(c_9c_{13} + c_8c_{14} + c_6c_{17}) - 2(c_9c_{15} + c_8c_{16}) \\
& \times (c_9c_{14} + c_8c_{15} + c_7c_{17}),
\end{aligned}$$

$$\begin{aligned}
d_{11} = & (c_3c_{16} + c_4c_{15})^2 + 2c_4c_{16}(c_2c_{16} + c_3c_{15} + c_4c_{14} + c_7c_{12}) \\
& - (c_4c_{17} - c_9c_{12})^2 \\
& - (c_9c_{15} + c_8c_{16})^2 - 2c_9c_{16}(c_9c_{14} + c_8c_{15} + c_7c_{17}),
\end{aligned}$$

$$d_{12} = 2c_4c_{16}(c_3c_{16} + c_4c_{15}) - 2c_9c_{16}(c_9c_{15} + c_8c_{16}),$$

$$d_{13} = (c_4c_{16})^2 - (c_9c_{16})^2.$$

Set

$$M_1(\varepsilon) = d_1\varepsilon^{12p} + d_2\varepsilon^{11p} + d_3\varepsilon^{10p} + d_4\varepsilon^{9p} + d_5\varepsilon^{8p} + d_6\varepsilon^{7p} \\ + d_7\varepsilon^{6p} + d_8\varepsilon^{5p} + d_9\varepsilon^{4p} + d_{10}\varepsilon^{3p} + d_{11}\varepsilon^{2p} + d_{12}\varepsilon^p + d_{13}. \quad (22)$$

and

$$M_2(\varepsilon) = d_1\varepsilon^{12} + d_2\varepsilon^{11p} + d_3\varepsilon^{10} + d_4\varepsilon^9 + d_5\varepsilon^8 + d_6\varepsilon^7 \\ + d_7\varepsilon^6 + d_8\varepsilon^5 + d_9\varepsilon^4 + d_{10}\varepsilon^3 + d_{11}\varepsilon^2 + d_{12}\varepsilon + d_{13}. \quad (23)$$

Lemma 3.1 (1) Assume that $b_3+b_5+b_7 \neq 0$ and $d_k > 0 (k = 1, 2, 3, \dots, 13)$, then Eq. (11) owns no root involving zero real part. (2) Assume that $d_{13} > 0$ and $\exists \varepsilon_0 > 0$ satisfying $M_2(\varepsilon_0) < 0$, then Eq. (11) owns at least two couples of purely imaginary roots.

Proof (1) It follows from (22) that

$$\frac{dM_1(\varepsilon)}{d\varepsilon} = 12pd_1\varepsilon^{12p-1} + 11pd_2\varepsilon^{11p-1} + 10pd_3\varepsilon^{10p-1} + 9pd_4\varepsilon^{9p-1} \\ + 8pd_5\varepsilon^{8p-1} + 7pd_6\varepsilon^{7p-1} + 6pd_7\varepsilon^{6p-1} + 5pd_8\varepsilon^{5p-1} \\ + 4pd_9\varepsilon^{4p-1} + 3pd_{10}\varepsilon^{3p-1} + 2pd_{11}\varepsilon^{2p-1} + pd_{12}\varepsilon^{p-1}. \quad (24)$$

Since $d_l > 0 (l = 1, 2, \dots, 12)$, one gains $\frac{dM_1(\varepsilon)}{d\varepsilon} > 0, \forall \varepsilon > 0$. In addition, $M_1(0) = d_{13} > 0$, one knows that Eq. (21) admits no positive real root. According to $b_3 + b_5 + b_7 \neq 0$, we can know that $s = 0$ is not the root of (11), which completes the proof of (1).

(2) Clearly, $M_2(0) = d_{13} > 0, M_2(\varepsilon_0) < 0 (\varepsilon_0 > 0)$ and $\lim_{\varepsilon \rightarrow +\infty} \frac{M_2(\varepsilon)}{d\varepsilon} = +\infty$, then there exist $\varepsilon_1 \in (0, \varepsilon_0)$ and $\varepsilon_2 \in (\varepsilon_0, +\infty)$ satisfying $M_2(\varepsilon_1) = M_2(\varepsilon_2) = 0$, then Eq.(21) owns at least two positive real roots. Then (11) owns at least two couples of purely imaginary roots, which completes the proof of (2). ■

Suppose that Eq.(21) owns twelve positive real roots $\varepsilon_i (i = 1, 2, \dots, 12)$. By (19), we get

$$\vartheta_j^k = \frac{1}{\varepsilon_j} \left[\arccos \left(-\frac{\Phi_3(\varepsilon_j)\Phi_5(\varepsilon_j) + \Phi_2(\varepsilon_j)\Phi_6(\varepsilon_j)}{\Phi_1(\varepsilon_j)\Phi_5(\varepsilon_j) + \Phi_2(\varepsilon_j)\Phi_4(\varepsilon_j)} \right) + 2l\pi \right], \quad (25)$$

where $l = 0, 1, 2, \dots, j = 1, 2, \dots, 12$. Let

$$\vartheta_0 = \min_{j=1,2,\dots,12} \{\vartheta_j^0\}, \varepsilon_0 = \varepsilon|_{\vartheta=\vartheta_0}. \quad (26)$$

Now we give the following condition:

$$(Q_3) \quad T_{1R}T_{2R} + T_{1I}T_{2I} > 0,$$

where

$$\begin{aligned} T_{1R} &= 3p\varepsilon_0^{3p-1} \cos \frac{(3p-1)\pi}{2} + 2pb_1\varepsilon_0^{2p-1} \cos \frac{(2p-1)\pi}{2} \\ &\quad + pb_2\varepsilon_0^{p-1} \cos \frac{(p-1)\pi}{2} + pb_4\varepsilon_0^{p-1} \cos \frac{(p-1)\pi}{2} \cos \varepsilon_0\vartheta_0 \\ &\quad + pb_4\varepsilon_0^{p-1} \sin \frac{(p-1)\pi}{2} \sin \varepsilon_0\vartheta_0 + pb_6\varepsilon_0^{p-1} \cos \frac{(p-1)\pi}{2} \\ &\quad \times \cos 2\varepsilon_0\vartheta_0 + pb_6\varepsilon_0^{p-1} \sin \frac{(p-1)\pi}{2} \sin 2\varepsilon_0\vartheta_0, \\ T_{1I} &= 3p\varepsilon_0^{3p-1} \sin \frac{(3p-1)\pi}{2} + 2pb_1\varepsilon_0^{2p-1} \sin \frac{(2p-1)\pi}{2} \\ &\quad + pb_2\varepsilon_0^{p-1} \sin \frac{(p-1)\pi}{2} - pb_4\varepsilon_0^{p-1} \cos \frac{(p-1)\pi}{2} \sin \varepsilon_0\vartheta_0 \\ &\quad + pb_4\varepsilon_0^{p-1} \sin \frac{(p-1)\pi}{2} \cos \varepsilon_0\vartheta_0 - pb_6\varepsilon_0^{p-1} \cos \frac{(p-1)\pi}{2} \\ &\quad \times \sin 2\varepsilon_0\vartheta_0 + pb_6\varepsilon_0^{p-1} \sin \frac{(p-1)\pi}{2} \cos 2\varepsilon_0\vartheta_0, \\ T_{2R} &= \left(b_4\varepsilon_0^p \cos \frac{p\pi}{2} + b_5\right) \varepsilon_0 \sin \varepsilon_0\vartheta_0 \\ &\quad - \left(b_4\varepsilon_0^p \sin \frac{p\pi}{2}\right) \varepsilon_0 \cos \varepsilon_0\vartheta_0 \\ &\quad + \left(b_6\varepsilon_0^p \cos \frac{p\pi}{2} + b_7\right) \varepsilon_0 \sin 2\varepsilon_0\vartheta_0 \\ &\quad - \left(b_6\varepsilon_0^p \sin \frac{p\pi}{2}\right) \varepsilon_0 \cos 2\varepsilon_0\vartheta_0, \\ T_{2I} &= \left(b_4\varepsilon_0^p \cos \frac{p\pi}{2} + b_5\right) \varepsilon_0 \cos \varepsilon_0\vartheta_0 \\ &\quad + \left(b_4\varepsilon_0^p \sin \frac{p\pi}{2}\right) \varepsilon_0 \sin \varepsilon_0\vartheta_0 \\ &\quad + \left(b_6\varepsilon_0^p \cos \frac{p\pi}{2} + b_7\right) \varepsilon_0 \cos 2\varepsilon_0\vartheta_0 \\ &\quad + \left(b_6\varepsilon_0^p \sin \frac{p\pi}{2}\right) \varepsilon_0 \sin 2\varepsilon_0\vartheta_0. \end{aligned}$$

Lemma 3.2. *Let $s(\vartheta) = \varsigma_1(\vartheta) + i\varsigma_2(\vartheta)$ be the root of Eq. (11) near $\vartheta = \vartheta_0$ satisfying $\varsigma_1(\vartheta_0) = 0, \varsigma_2(\vartheta_0) = \varepsilon_0$, then $\operatorname{Re} \left(\frac{ds}{d\vartheta} \right) \Big|_{\vartheta=\vartheta_0, \varepsilon=\varepsilon_0} > 0$.*

Proof It follows from Eq.(11) that

$$\begin{aligned} & (3ps^{3p-1} + 2pb_1s^{2p-1} + pb_2s^{p-1}) \frac{ds}{d\vartheta} + pb_4s^{p-1}e^{-s\vartheta} \frac{ds}{d\vartheta} \\ & - e^{-s\vartheta} \left(\frac{ds}{d\vartheta} \vartheta + s \right) (b_4s^p + b_5) + pb_6s^{p-1}e^{-2s\vartheta} \frac{ds}{d\vartheta} \\ & - 2e^{-2s\vartheta} (b_6s^p + b_7) \left(\frac{ds}{d\vartheta} \theta + s \right) = 0, \end{aligned} \quad (27)$$

which results in

$$\left(\frac{ds}{d\vartheta} \right)^{-1} = \frac{T_1(s)}{T_2(s)} - \frac{\vartheta}{s}, \quad (28)$$

where

$$\begin{cases} T_1(s) = 3ps^{3p-1} + 2pb_1s^{2p-1} + pb_2s^{p-1} \\ \quad + pb_4s^{p-1}e^{-s\vartheta} + pb_6s^{p-1}e^{-2s\vartheta}, \\ T_2(s) = se^{-s\vartheta} (b_4s^p + b_5) + 2se^{-2s\vartheta} (b_6s^p + b_7). \end{cases} \quad (29)$$

Then

$$\operatorname{Re} \left[\left(\frac{ds}{d\vartheta} \right)^{-1} \right]_{\vartheta=\vartheta_0, \varepsilon=\varepsilon_0} = \operatorname{Re} \left[\frac{T_1(s)}{T_2(s)} \right]_{\vartheta=\vartheta_0, \varepsilon=\varepsilon_0} = \frac{T_{1R}T_{2R} + T_{1I}T_{2I}}{T_{2R}^2 + T_{2I}^2}. \quad (30)$$

In view of (Q_3) , we gain

$$\operatorname{Re} \left[\left(\frac{ds}{d\vartheta} \right)^{-1} \right]_{\vartheta=\vartheta_0, \varepsilon=\varepsilon_0} > 0. \quad (31)$$

The proof completes. ■

Applying Lemma 2.1, the following assertion can be lightly is acquired.

Theorem 3.1. *If (Q_1) - (Q_3) are fulfilled, then $W(w_{1*}, w_{2*}, w_{3*})$ of system (5) keeps locally asymptotically stability when $\vartheta \in [0, \vartheta_0)$ and a cluster of Hopf bifurcations of system (5) happen near $W(w_{1*}, w_{2*}, w_{3*})$ when $\vartheta = \vartheta_0$.*

4 Bifurcation control via extended hybrid controller

In this section, we are to use a novel extended hybrid controller which includes a common hybrid controller that consists of state feedback and parameter perturbation and a PD controller to control the stability and Hopf bifurcation for model (5). Following the ideas of [49, 50] and [51], we get the following fractional-order controlled delayed turbidostat model:

$$\left\{ \begin{array}{l} \frac{d^p w_1(t)}{dt^p} = [a + \kappa_1 w_2(t - \vartheta) + \kappa_2 w_3(t - \vartheta)](w_0 - w_1) \\ \quad - \frac{w_2}{\gamma_1} g_1(w_1) - \frac{w_3}{\gamma_2} g_2(w_1), \\ \frac{d^p w_2(t)}{dt^p} = \rho_1 \{w_2 [g_1(w_1) - (a + \kappa_1 w_2(t - \vartheta) + \kappa_2 w_3(t - \vartheta))] \} \\ \quad + \rho_2 [w_2(t - \vartheta) - w_2], \\ \frac{d^p w_3(t)}{dt^p} = w_3 [g_2(w_1) - (a + \kappa_1 w_2(t - \vartheta) + \kappa_2 w_3(t - \vartheta))] \\ \quad + \tau_p [w_3 - w_{3*}] + \tau_d \frac{d^p [w_3 - w_{3*}]}{dt^p}, \end{array} \right. \quad (32)$$

where ρ_1, ρ_2 stands for feedback gain parameters and $\tau_p, \tau_d \neq 1$ stand for the proportional control parameter and the derivative parameter, respectively. Clearly, model (32) and model (5) admit the same positive equilibrium point $W(w_{1*}, w_{2*}, w_{3*})$. The linear system of system (5) at $W(w_{1*}, w_{2*}, w_{3*})$ owns the following form:

$$\mathcal{D}^p w(t) = C_1 w(t) + C_2 w(t - \theta), \quad (33)$$

where

$$w(t) = \begin{bmatrix} w_1(t) \\ w_2(t) \\ w_3(t) \end{bmatrix}, C_1 = \begin{bmatrix} \alpha_1 & \alpha_2 & \alpha_3 \\ \alpha_4 & \alpha_5 & 0 \\ \alpha_6 & 0 & \alpha_7 \end{bmatrix}, C_2 = \begin{bmatrix} 0 & \beta_1 & \beta_2 \\ 0 & \beta_3 & \beta_4 \\ 0 & \beta_5 & \beta_6 \end{bmatrix}, \quad (34)$$

where

$$\left\{ \begin{array}{l} \alpha_1 = - \left[a + \kappa_1 w_{2*} + \kappa_{3*} + \frac{g'_1(w_{1*})}{\gamma_1} + \frac{g'_2(w_{1*})}{\gamma_2} \right], \\ \alpha_2 = - \frac{g_1(w_{1*}) + g'_1(w_{1*})}{\gamma_1}, \\ \alpha_3 = - \frac{g_2(w_{1*}) + g'_2(w_{1*})}{\gamma_2}, \\ \alpha_4 = \rho_1 w_{2*} g'_1(w_{1*}), \alpha_5 = -\rho_2, \\ \alpha_6 = \frac{w_{3*} g'_2(w_{1*})}{1 - \tau_d}, \alpha_7 = \frac{\tau_p}{1 - \tau_d}, \\ \beta_1 = \kappa_1 (w_0 - w_{1*}), \beta_2 = \kappa_2 (w_0 - w_{1*}), \\ \beta_3 = -\kappa_1 w_{2*} + \rho_2, \beta_4 = -\kappa_2 w_{2*}, \\ \beta_5 = -\frac{\kappa_1 w_{3*}}{1 - \tau_d}, \beta_6 = -\frac{\kappa_2 w_{3*}}{1 - \tau_d}. \end{array} \right. \quad (35)$$

The characteristic equation of system (33) reads as

$$\det \begin{bmatrix} s^p - \alpha_1 & -\alpha_2 - \beta_1 e^{-s\vartheta} & -\alpha_3 - \beta_2 e^{-s\vartheta} \\ -\alpha_4 & s^p - \alpha_5 - \beta_3 e^{-s\vartheta} & -\beta_4 e^{-s\vartheta} \\ -\alpha_5 & -\beta_5 e^{-s\vartheta} & s^p - \alpha_7 - \beta_6 e^{-s\vartheta} \end{bmatrix} = 0, \quad (36)$$

which results in

$$s^{3p} + e_1 s^{2p} + e_2 s^p + e_3 + (e_4 s^p + e_5) e^{-s\vartheta} + (e_6 s^p + e_7) e^{-2s\vartheta} = 0, \quad (37)$$

where

$$\left\{ \begin{array}{l} e_1 = \alpha_7 \beta_3 - \beta_3 - 2\alpha_1 - \alpha_5, \\ e_2 = \alpha_1 \alpha_7 + \alpha_5 \alpha_7 + \alpha_1 \alpha_5 - \alpha_3 \alpha_5 - \alpha_2 \alpha_4 \\ \quad + \alpha_7 \beta_3 + \alpha_1 \beta_3 + \beta_6 (\alpha_1 + \alpha_5), \\ e_3 = \alpha_3 \alpha_5^2 - \alpha_1 \alpha_5 \alpha_7 + \alpha_4 \alpha_7 \beta_1 + \alpha_2 \alpha_4 \alpha_7, \\ e_4 = -(\alpha_5 \beta_2 + \alpha_4 \beta_1), \\ e_5 = -(\alpha_1 \alpha_5 \beta_6 + \alpha_1 \alpha_7 \beta_3 + \alpha_2 \alpha_5 \beta_4 + \alpha_3 \alpha_4 \beta_5 \\ \quad - \alpha_3 \alpha_5 \beta_3 - \alpha_2 \alpha_4 \beta_6), \\ e_6 = \beta_3 \beta_6 - \beta_4 \beta_5, \\ e_7 = \alpha_1 \beta_4 \beta_5 - \alpha_1 \beta_3 \beta_6 - \alpha_4 \beta_2 \beta_5 + \alpha_5 \beta_2 \beta_3 + \alpha_4 \beta_1 \beta_6. \end{array} \right. \quad (38)$$

When $\theta = 0$, then Eq.(37) has the following form:

$$\lambda^3 + e_1\lambda^2 + (e_2 + e_4 + e_6)\lambda + e_3 + e_5 + e_7 = 0. \tag{39}$$

If

$$(Q_4) \begin{cases} \Lambda_1 = e_1 > 0, \\ \Lambda_2 = \det \begin{bmatrix} e_1 & 1 \\ e_3 + e_5 + e_7 & e_2 + e_4 + e_6 \end{bmatrix}, \\ \Lambda_3 = (e_3 + e_5 + e_7)\Delta_2 > 0 \end{cases}$$

is fulfilled, then the three roots $\lambda_1, \lambda_2, \lambda_3$ of Eq. (39) obey $|\arg(\lambda_1)| > \frac{p\pi}{2}, |\arg(\lambda_2)| > \frac{p\pi}{2}, |\arg(\lambda_3)| > \frac{p\pi}{2}$. In view of Lemma 2.1, we can understand that the positive equilibrium point $W(w_{1*}, w_{2*}, w_{3*})$ of system (35) with the delay $\vartheta = 0$ maintains locally asymptotically stability.

By (37), we have

$$(s^{3p} + e_1s^{2p} + e_2s^p + e_3)e^{s\vartheta} + (e_4s^p + e_5) + (e_6s^p + e_7)e^{-s\vartheta} = 0. \tag{40}$$

Suppose that $s = i\epsilon = \epsilon \left(\cos \frac{\pi}{2} + i \sin \frac{\pi}{2} \right)$ is the root of Eq. (40). Then by Eq.(40), one gains

$$\begin{aligned} & \left[\epsilon^{3p} \left(\cos \frac{3p\pi}{2} + i \sin \frac{3p\pi}{2} \right) + e_1\epsilon^{2p}(\cos p\pi + i \sin p\pi) \right. \\ & \left. + e_2\epsilon^p \left(\cos \frac{p\pi}{2} + i \sin \frac{p\pi}{2} \right) + e_3 \right] (\cos \epsilon\vartheta + i \sin \epsilon\vartheta) \\ & + \left[e_4\epsilon^p \left(\cos \frac{p\pi}{2} + i \sin \frac{p\pi}{2} \right) + e_5 \right] \\ & + \left[e_6\epsilon^p \left(\cos \frac{p\pi}{2} + i \sin \frac{p\pi}{2} \right) + e_7 \right] (\cos \epsilon\vartheta - i \sin \epsilon\vartheta) = 0. \tag{41} \end{aligned}$$

Then it follows from (41) that

$$\begin{cases} \Psi_1(\epsilon) \cos \epsilon\vartheta - \Psi_2(\epsilon) \sin \epsilon\vartheta = -\Psi_3(\epsilon), \\ \Psi_4(\epsilon) \cos \epsilon\vartheta + \Psi_5(\epsilon) \sin \epsilon\vartheta = -\Psi_6(\epsilon), \end{cases} \tag{42}$$

where

$$\left\{ \begin{array}{l} \Psi_1(\epsilon) = f_1\epsilon^{3p} + f_2\epsilon^{2p} + f_3\epsilon^p + f_4, \\ \Psi_2(\epsilon) = f_5\epsilon^{3p} + f_6\epsilon^{2p} + f_7\epsilon^p, \\ \Psi_3(\epsilon) = f_8\epsilon^p + f_9, \\ \Psi_4(\epsilon) = f_{10}\epsilon^{3p} + f_{11}\epsilon^{2p} + f_{12}\epsilon^p, \\ \Psi_5(\epsilon) = f_{13}\epsilon^{3p} + f_{14}\epsilon^{2p} + f_{15}\epsilon^p + f_{16}, \\ \Psi_6(\epsilon) = f_{17}\epsilon^p, \end{array} \right. \quad (43)$$

where

$$\left\{ \begin{array}{l} f_1 = \cos \frac{3p\pi}{2}, \\ f_2 = e_1 \cos p\pi, \\ f_3 = (e_2 + e_6) \cos \frac{p\pi}{2}, \\ f_4 = e_3 + e_7, \\ f_5 = \sin \frac{3p\pi}{2}, \\ f_6 = e_1 \sin p\pi, \\ f_7 = (e_2 - e_6) \sin \frac{p\pi}{2}, \\ f_8 = e_4 \cos \frac{p\pi}{2}, \\ f_9 = e_5, \\ f_{10} = \sin \frac{3p\pi}{2}, \\ f_{11} = e_1 \sin p\pi, \\ f_{12} = (e_2 + e_6) \sin \frac{p\pi}{2}, \\ f_{13} = \cos \frac{3p\pi}{2}, \\ f_{14} = e_1 \cos p\pi, \\ f_{15} = (e_2 - e_6) \cos \frac{p\pi}{2}, \\ f_{16} = e_3 - e_7, \\ f_{17} = e_4 \sin \frac{p\pi}{2}. \end{array} \right. \quad (44)$$

By (42), we have

$$\left\{ \begin{array}{l} \cos \epsilon\vartheta = -\frac{\Psi_3(\epsilon)\Psi_5(\epsilon) + \Psi_2(\epsilon)\Psi_6(\epsilon)}{\Psi_1(\epsilon)\Psi_5(\epsilon) + \Psi_2(\epsilon)\Psi_4(\epsilon)}, \\ \sin \epsilon\vartheta = \frac{\Psi_1(\epsilon)\Psi_6(\epsilon) - \Psi_3(\epsilon)\Psi_4(\epsilon)}{\Psi_1(\epsilon)\Psi_5(\epsilon) + \Psi_2(\epsilon)\Psi_4(\epsilon)}. \end{array} \right. \quad (45)$$

In view of $\cos^2 \epsilon\vartheta + \sin^2 \epsilon\vartheta = 1$, it follows from (45) that

$$\begin{aligned} & [\Psi_3(\epsilon)\Psi_5(\epsilon) + \Psi_2(\epsilon)\Psi_6(\epsilon)]^2 + [\Psi_1(\epsilon)\Psi_6(\epsilon) - \Psi_3(\epsilon)\Psi_4(\epsilon)]^2 \\ &= [\Psi_1(\epsilon)\Psi_5(\epsilon) + \Psi_2(\epsilon)\Psi_4(\epsilon)]^2, \end{aligned} \quad (46)$$

which results in

$$\begin{aligned} & g_1\epsilon^{12p} + g_2\epsilon^{11p} + g_3\epsilon^{10p} + g_4\epsilon^{9p} + g_5\epsilon^{8p} + g_6\epsilon^{7p} + g_7\epsilon^{6p} \\ &+ g_8\epsilon^{5p} + g_9\epsilon^{4p} + g_{10}\epsilon^{3p} + g_{11}\epsilon^{2p} + g_{12}\epsilon^p + g_{13} = 0, \end{aligned} \quad (47)$$

where

$$\begin{aligned} g_1 &= (f_1f_{13} + f_5f_{10})^2, \\ g_2 &= 2(f_1f_{13} + f_5f_{10})(f_1f_{14} + f_2f_{13} + f_5f_{11} + f_6f_{10}) \\ g_3 &= (f_1f_{14} + f_2f_{13} + f_5f_{11} + f_6f_{10})^2 - 2(f_1f_{13} + f_5f_{10}) \\ &\quad \times (f_1f_{15} + f_2f_{14} + f_3f_{13} + f_5f_{12} + f_6f_{11} + f_7f_{10}), \\ g_4 &= 2(f_1f_{13} + f_5f_{10})(f_1f_{16} + f_2f_{15} + f_3f_{14} + f_6f_{12} + f_7f_{11}) \\ &\quad + 2(f_1f_{14} + f_2f_{13} + f_5f_{11} + f_6f_{10})(f_1f_{15} + f_2f_{14} + f_3f_{13} \\ &\quad + f_5f_{12} + f_6f_{11} + f_7f_{10}), \\ g_5 &= (f_1f_{15} + f_2f_{14} + f_3f_{13} + f_5f_{12} + f_6f_{11} + f_7f_{10})^2 \\ &\quad + 2(f_1f_{13} + f_5f_{10})(f_2f_{16} + f_3f_{15} + f_4f_{14} + f_7f_{12}) \\ &\quad + 2(f_1f_{14} + f_2f_{13} + f_5f_{11} + f_6f_{10})(f_1f_{16} + f_2f_{15} \\ &\quad + f_3f_{14} + f_4f_{13} + f_6f_{12} + f_7f_{11}) - (f_1f_{17} - f_8f_{10})^2 \\ &\quad - (f_8f_{13})^2, \\ g_6 &= 2(f_1f_{13} + f_5f_{10})(f_3f_{16} + f_4f_{15}) + 2(f_1f_{14} + f_2f_{13} \\ &\quad + f_5f_{11} + f_6f_{10})(f_2f_{16} + f_3f_{15} + f_4f_{14} + f_7f_{12}) \\ &\quad + 2(f_1f_{15} + f_2f_{14} + f_3f_{13} + f_5f_{12} + f_6f_{11} + f_7f_{10}) \\ &\quad \times (f_1f_{16} + f_2f_{15} + f_3f_{14} + f_4f_{13} + f_6f_{12} + f_7f_{11}) \\ &\quad - 2(f_1f_{17} - f_8f_{10})(f_2f_{17} - f_9f_{10} - f_8f_{11}) \\ &\quad - 2f_8f_{13}(f_9f_{13} + f_8f_{14} + f_6f_{17}), \end{aligned}$$

$$\begin{aligned}
g_7 &= (f_1 f_{16} + f_2 f_{15} + f_3 f_{14} + f_4 f_{13} + f_6 f_{12} + f_7 f_{11})^2 \\
&\quad + 2f_4 f_{16}(f_1 f_{13} + f_5 f_{10}) + 2(f_3 f_{16} + f_4 f_{15})(f_1 f_{14} + f_2 f_{13} \\
&\quad + f_5 f_{11} + f_6 f_{10}) + 2(f_1 f_{15} + f_2 f_{14} + f_3 f_{13} \\
&\quad + f_5 f_{12} + f_6 f_{11} + f_7 f_{10})(f_2 f_{16} + f_3 f_{15} + f_4 f_{14} + f_7 f_{12}) \\
&\quad - (f_2 f_{17} - f_9 f_{10} - f_8 f_{11})^2 - (f_9 f_{13} + f_8 f_{14} + f_6 f_{17})^2 \\
&\quad - 2f_8 f_{13}(f_9 f_{14} + f_8 f_{15} + f_7 f_{17}), \\
g_8 &= 2f_4 f_6(f_1 f_{14} + f_2 f_{13} + f_5 f_{11} + f_6 f_{10}) + 2(f_1 f_{15} + f_2 f_{14} \\
&\quad + f_3 f_{13} + f_5 f_{12} + f_6 f_{11} + f_7 f_{10})(f_3 f_{16} + f_4 f_{15}) \\
&\quad + 2(f_1 f_{16} + f_2 f_{15} + f_3 f_{14} + f_4 f_{13} + f_6 f_{12} + f_7 f_{11}) \\
&\quad \times (f_2 f_{16} + f_3 f_{15} + f_4 f_{14} + f_7 f_{12}) - 2(f_1 f_{17} \\
&\quad - f_8 f_{10})(f_4 f_{17} - f_9 f_{12}) - 2(f_2 f_{17} - f_9 f_{10} - f_8 f_{11}) \\
&\quad \times (f_3 f_{17} - f_9 f_{11} - f_8 f_{12}) - 2f_8 f_{13}(f_9 f_{15} + f_8 f_{16}) \\
&\quad - 2(f_9 f_{13} + f_8 f_{14} + f_6 f_{17})(f_9 f_{14} + f_8 f_{15} + f_7 f_{17}), \\
g_9 &= (f_2 f_{16} + f_3 f_{15} + f_4 f_{14} + f_7 f_{12})^2 + 2(f_3 f_{16} + f_4 f_{15}) \\
&\quad \times (f_1 f_{16} + f_2 f_{15} + f_3 f_{14} + f_4 f_{13} + f_6 f_{12} + f_7 f_{11}) \\
&\quad + 2f_4 f_{16}(f_1 f_{15} + f_2 f_{14} + f_3 f_{13} + f_5 f_{12} + f_6 f_{11} + f_7 f_{10}) \\
&\quad - (f_3 f_{17} - f_9 f_{11} - f_8 f_{12})^2 - 2(f_2 f_{17} - f_9 f_{10} - f_8 f_{11}) \\
&\quad \times (f_4 f_{17} - f_9 f_{12}) - (f_9 f_{14} + f_8 f_{15} + f_7 f_{17})^2 \\
&\quad - 2(f_9 f_{15} + f_8 f_{16})(f_9 f_{13} + f_8 f_{14} + f_6 f_{17}), \\
g_{10} &= 2f_4 f_{16}(f_1 f_{16} + f_2 f_{15} + f_3 f_{14} + f_4 f_{13} + f_6 f_{12} + f_7 f_{11}) \\
&\quad + 2(f_3 f_{16} + f_4 f_{15})(f_2 f_{16} + f_3 f_{15} + f_4 f_{14} + f_7 f_{12}) \\
&\quad - 2(f_3 f_{17} - f_9 f_{11} - f_8 f_{12})(f_4 f_{17} - f_9 f_{12}) \\
&\quad - 2f_9 f_{16}(f_9 f_{13} + f_8 f_{14} + f_6 f_{17}) - 2(f_9 f_{15} + f_8 f_{16}) \\
&\quad \times (f_9 f_{14} + f_8 f_{15} + f_7 f_{17}), \\
g_{11} &= (f_3 f_{16} + f_4 f_{15})^2 + 2f_4 f_{16}(f_2 f_{16} + f_3 f_{15} + f_4 f_{14} + f_7 f_{12}) \\
&\quad - (f_4 f_{17} - f_9 f_{12})^2 \\
&\quad - (f_9 f_{15} + f_8 f_{16})^2 - 2f_9 f_{16}(f_9 f_{14} + f_8 f_{15} + f_7 f_{17}), \\
g_{12} &= 2f_4 f_{16}(f_3 f_{16} + f_4 f_{15}) - 2f_9 f_{16}(f_9 f_{15} + f_8 f_{16}), \\
g_{13} &= (f_4 f_{16})^2 - (f_9 f_{16})^2.
\end{aligned}$$

Set

$$N_1(\epsilon) = g_1\epsilon^{12p} + g_2\epsilon^{11p} + g_3\epsilon^{10p} + g_4\epsilon^{9p} + d_5\epsilon^{8p} + g_6\epsilon^{7p} + g_7\epsilon^{6p} + g_8\epsilon^{5p} + g_9\epsilon^{4p} + g_{10}\epsilon^{3p} + g_{11}\epsilon^{2p} + g_{12}\epsilon^p + g_{13}, \tag{48}$$

and

$$N_2(\epsilon) = g_1\epsilon^{12} + g_2\epsilon^{11} + g_3\epsilon^{10} + g_4\epsilon^9 + d_5\epsilon^8 + g_6\epsilon^7 + g_7\epsilon^6 + g_8\epsilon^5 + g_9\epsilon^4 + g_{10}\epsilon^3 + g_{11}\epsilon^2 + g_{12}\epsilon + g_{13}, \tag{49}$$

Lemma 4.1 (1) Assume that $e_3 + e_5 + e_7 \neq 0$ and $g_k > 0 (k = 1, 2, 3, \dots, 13)$, then Eq. (37) owns no root involving zero real part. (2) Assume that $g_{13} > 0$ and $\exists \epsilon_0 > 0$ satisfying $N_2(\epsilon_0) < 0$, then Eq. (37) owns at least two couples of purely imaginary roots.

Proof (1) It follows from (48) that

$$\begin{aligned} \frac{dN_1(\epsilon)}{d\epsilon} &= 12pg_1\epsilon^{12p-1} + 11pg_2\epsilon^{11p-1} + 10pg_3\epsilon^{10p-1} + 9pg_4\epsilon^{9p-1} \\ &\quad + 8pg_5\epsilon^{8p-1} + 7pg_6\epsilon^{7p-1} + 6pg_7\epsilon^{6p-1} + 5pg_8\epsilon^{5p-1} \\ &\quad + 4pg_9\epsilon^{4p-1} + 3pg_{10}\epsilon^{3p-1} + 2pg_{11}\epsilon^{2p-1} + pg_{12}\epsilon^{p-1}. \end{aligned} \tag{50}$$

Since $g_l > 0 (l = 1, 2, \dots, 12)$, one gains $\frac{dN_1(\epsilon)}{d\epsilon} > 0, \forall \epsilon > 0$. In addition, $N_1(0) = g_{13} > 0$, one knows that Eq. (47) admits no positive real root. According to $e_3 + e_5 + e_7 \neq 0$, we can know that $s = 0$ is not the root of (37), which completes the proof of (1).

(2) Clearly, $N_2(0) = g_{13} > 0, N_2(\epsilon_0) < 0 (\epsilon_0 > 0)$ and $\lim_{\epsilon \rightarrow +\infty} \frac{N_2(\epsilon)}{d\epsilon} = +\infty$, then there exist $\epsilon_1 \in (0, \epsilon_0)$ and $\epsilon_2 \in (\epsilon_0, +\infty)$ satisfying $N_2(\epsilon_1) = N_2(\epsilon_2) = 0$, then Eq.(47) owns at least two positive real roots. Then (37) owns at least two couples of purely imaginary roots, which completes the proof of (2). ■

Suppose that Eq.(47) owns twelve positive real roots $\epsilon_i (i = 1, 2, \dots, 12)$. By (42), we get

$$\vartheta_i^k = \frac{1}{\epsilon_j} \left[\arccos \left(-\frac{\Psi_3(\epsilon)\Psi_5(\epsilon) + \Psi_2(\epsilon)\Psi_6(\epsilon)}{\Psi_1(\epsilon)\Psi_5(\epsilon) + \Psi_2(\epsilon)\Psi_4(\epsilon)} \right) + 2k\pi \right], \tag{51}$$

where $k = 0, 1, 2, \dots, i = 1, 2, \dots, 12$. Let

$$\vartheta_* = \min_{i=1,2,\dots,12} \{\vartheta_i^0\}, \epsilon_0 = \epsilon|_{\vartheta=\vartheta_*}. \quad (52)$$

Now we give the following condition:

$$(Q_5) \quad S_{1R}S_{2R} + S_{1I}S_{2I} > 0,$$

where

$$\left\{ \begin{array}{l} S_{1R} = 3pe_0^{3p-1} \cos \frac{(3p-1)\pi}{2} + 2pe_1\epsilon_0^{2p-1} \cos \frac{(2p-1)\pi}{2} \\ \quad + pe_2\epsilon_0^{p-1} \cos \frac{(p-1)\pi}{2} + pe_4\epsilon_0^{p-1} \cos \frac{(p-1)\pi}{2} \cos \epsilon_0\vartheta_* \\ \quad + pe_4\epsilon_0^{p-1} \sin \frac{(p-1)\pi}{2} \sin \epsilon_0\vartheta_* + pe_6\epsilon_0^{p-1} \cos \frac{(p-1)\pi}{2} \\ \quad \times \cos 2\epsilon_0\vartheta_* + pe_6\epsilon_0^{p-1} \sin \frac{(p-1)\pi}{2} \sin 2\epsilon_0\vartheta_*, \\ S_{1I} = 3pe_0^{3p-1} \sin \frac{(3p-1)\pi}{2} + 2pe_1\epsilon_0^{2p-1} \sin \frac{(2p-1)\pi}{2} \\ \quad + pe_2\epsilon_0^{p-1} \sin \frac{(p-1)\pi}{2} - pe_4\epsilon_0^{p-1} \cos \frac{(p-1)\pi}{2} \sin \epsilon_0\vartheta_* \\ \quad + pe_4\epsilon_0^{p-1} \sin \frac{(p-1)\pi}{2} \cos \epsilon_0\vartheta_* - pe_6\epsilon_0^{p-1} \cos \frac{(p-1)\pi}{2} \\ \quad \times \sin 2\epsilon_0\vartheta_* + pe_6\epsilon_0^{p-1} \sin \frac{(p-1)\pi}{2} \cos 2\epsilon_0\vartheta_*, \\ S_{2R} = \left(e_4\epsilon_0^p \cos \frac{p\pi}{2} + e_5 \right) \epsilon_0 \sin \epsilon_0\vartheta_* - \left(e_4\epsilon_0^p \sin \frac{p\pi}{2} \right) \\ \quad \times \epsilon_0 \cos \epsilon_0\vartheta_* + \left(e_6\epsilon_0^p \cos \frac{p\pi}{2} + e_7 \right) \epsilon_0 \sin 2\epsilon_0\vartheta_* \\ \quad - \left(e_6\epsilon_0^p \sin \frac{p\pi}{2} \right) \epsilon_0 \cos 2\epsilon_0\vartheta_*, \\ S_{2I} = \left(e_4\epsilon_0^p \cos \frac{p\pi}{2} + e_5 \right) \epsilon_0 \cos \epsilon_0\vartheta_* + \left(e_4\epsilon_0^p \sin \frac{p\pi}{2} \right) \\ \quad \times \epsilon_0 \sin \epsilon_0\vartheta_* + \left(e_6\epsilon_0^p \cos \frac{p\pi}{2} + e_7 \right) \epsilon_0 \cos 2\epsilon_0\vartheta_* \\ \quad + \left(e_6\epsilon_0^p \sin \frac{p\pi}{2} \right) \epsilon_0 \sin 2\epsilon_0\vartheta_*. \end{array} \right. \quad (53)$$

Lemma 4.2. Let $s(\vartheta) = \eta_1(\vartheta) + i\eta_2(\vartheta)$ be the root of Eq. (37) near $\vartheta = \vartheta_*$ satisfying $\eta_1(\vartheta_*) = 0, \eta_2(\vartheta_*) = \epsilon_0$, then $\operatorname{Re} \left(\frac{ds}{d\vartheta} \right) \Big|_{\vartheta=\vartheta_*, \epsilon=\epsilon_0} > 0$.

Proof It follows from Eq.(37) that

$$\begin{aligned} & (3ps^{3p-1} + 2pe_1s^{2p-1} + pe_2s^{p-1}) \frac{ds}{d\vartheta} + pe_4s^{p-1}e^{-s\vartheta} \frac{ds}{d\vartheta} \\ & - e^{-s\vartheta} \left(\frac{ds}{d\vartheta} \vartheta + s \right) (e_4s^p + e_5) + pe_6s^{p-1}e^{-2s\vartheta} \frac{ds}{d\vartheta} \\ & - 2e^{-2s\vartheta} (e_6s^p + e_7) \left(\frac{ds}{d\vartheta} \theta + s \right) = 0, \end{aligned} \quad (54)$$

which results in

$$\left(\frac{ds}{d\vartheta} \right)^{-1} = \frac{S_1(s)}{S_2(s)} - \frac{\vartheta}{s}, \quad (55)$$

where

$$\begin{cases} S_1(s) = 3ps^{3p-1} + 2pe_1s^{2p-1} + pe_2s^{p-1} \\ \quad + pe_4s^{p-1}e^{-s\vartheta} + pe_6s^{p-1}e^{-2s\vartheta}, \\ S_2(s) = se^{-s\vartheta} (e_4s^p + e_5) + 2se^{-2s\vartheta} (e_6s^p + e_7). \end{cases} \quad (56)$$

Then

$$\operatorname{Re} \left[\left(\frac{ds}{d\vartheta} \right)^{-1} \right]_{\vartheta=\vartheta_*, \epsilon=\epsilon_0} = \operatorname{Re} \left[\frac{S_1(s)}{S_2(s)} \right]_{\vartheta=\vartheta_*, \epsilon=\epsilon_0} = \frac{S_{1R}S_{2R} + S_{1I}S_{2I}}{S_{2R}^2 + S_{2I}^2}. \quad (57)$$

In view of (Q_5) , we gain

$$\operatorname{Re} \left[\left(\frac{ds}{d\vartheta} \right)^{-1} \right]_{\vartheta=\vartheta_*, \epsilon=\epsilon_0} > 0. \quad (58)$$

The proof completes. ■

Applying Lemma 2.1, the following assertion can be lightly is acquired.

Theorem 4.1. *If $(Q_1), (Q_4), (Q_5)$ are fulfilled, then $W(w_{1*}, w_{2*}, w_{3*})$ of system (32) keeps locally asymptotically stability when $\vartheta \in [0, \vartheta_*)$ and a cluster of Hopf bifurcations of system (35) happen near $W(w_{1*}, w_{2*}, w_{3*})$ when $\vartheta = \vartheta_*$.*

Remark 4.1. *In model (5), there is only delay. If there are two different delays or multiple delays, we can also investigate the bifurcation issue of model (5). We will leave it for future work.*

Remark 4.2. *In this paper, some assumptions (for example, $(Q_3), (Q_5)$,*

etc.) are very complex. But we can check the correctness of these assumptions by virtue of computer.

Remark 4.3. In this paper, we have used an extended hybrid controller to control stability and Hopf bifurcation. Of course, we can adopt other controllers to explore this topic. We leave it for future work.

5 Software experiments

Example 5.1. Give the fractional-order delayed turbidostat model as follows:

$$\left\{ \begin{array}{l} \frac{d^p w_1(t)}{dt^p} = [a + \kappa_1 w_2(t - \vartheta) + \kappa_2 w_3(t - \vartheta)](w_0 - w_1) \\ \quad - \frac{w_2}{\gamma_1} g_1(w_1) - \frac{w_3}{\gamma_2} g_2(w_1), \\ \frac{d^p w_2(t)}{dt^p} = w_2 [g_1(w_1) - (a + \kappa_1 w_2(t - \vartheta) + \kappa_2 w_3(t - \vartheta))], \\ \frac{d^p w_3(t)}{dt^p} = w_3 [g_2(w_1) - (a + \kappa_1 w_2(t - \vartheta) + \kappa_2 w_3(t - \vartheta))], \end{array} \right. \quad (59)$$

where $p = 0.93$, $a = 1.4$, $\kappa_1 = 2.2$, $\kappa_2 = 1.05$, $w_0 = 1$, $\gamma_1 = 1$, $\gamma_2 = 1$, $g_1(w_1) = \frac{3w_1}{0.25+w_2}$, $g_2(w_1) = \frac{5w_1}{0.8+w_2}$. We can easily obtain that system (59) owns the unique positive equilibrium point $W(w_{1*}, w_{2*}, w_{3*}) = W(0.5750, 0.2127, 0.2123)$. The three assumptions (Q_1) , (Q_2) , (Q_3) of Theorem 3.1 are fulfilled. With the aid of Matlab software, one can get $\varepsilon_0 = 3.4456$, $\vartheta_0 = 1.91$. To check the correctness of the main conclusions of Theorem 3.1, we take two delays as examples. Firstly, select $\vartheta = 1.82$ which means $\vartheta < \vartheta_0 = 1.91$, that is to say, ϑ falls into the range $[0, \vartheta_0)$. To this case, the Matlab simulation figures are displayed in Figure 1. Obviously, Figure 1 manifests that the limiting nutrient concentration w_1 will be closed to 0.5750, the concentration of the first competitor w_2 will be closed to 0.2127 and the concentration of the second competitor w_3 will be closed to 0.2123 as $t \rightarrow +\infty$. Secondly, choose $\vartheta = 2.13$ which means $\vartheta > \vartheta_0 = 1.91$, that is to say, ϑ exceeds the threshold delay number ϑ_0 . To this case, the Matlab simulation figures are displayed in Figure 2. Obviously, Figure 2 manifests that the limiting nutrient concentration w_1 is about to remain a periodic oscillation state around 0.5750, the concen-

tration of the first competitor w_2 is about to remain a periodic oscillation state around 0.2127 and the concentration of the second competitor w_3 is about to remain a periodic oscillation state around 0.2123. That is to say, system (59) are to produce a limit cycle (namely, Hopf bifurcation) near $W(w_{1*}, w_{2*}, w_{3*}) = W(0.5750, 0.2127, 0.2123)$. Furthermore, the bifurcation figures of system (59) are provided to embody the bifurcation point $\vartheta_0 = 1.91$ (see Figures 3-5).

Example 5.2. Give the fractional-order controlled delayed turbidostat model as follows:

$$\left\{ \begin{array}{l} \frac{d^p w_1(t)}{dt^p} = [a + \kappa_1 w_2(t - \vartheta) + \kappa_2 w_3(t - \vartheta)](w_0 - w_1) \\ \quad - \frac{w_2}{\gamma_1} g_1(w_1) - \frac{w_3}{\gamma_2} g_2(w_1), \\ \frac{d^p w_2(t)}{dt^p} = \rho_1 \{w_2 [g_1(w_1) - (a + \kappa_1 w_2(t - \vartheta) + \kappa_2 w_3(t - \vartheta))] \} \\ \quad + \rho_2 [w_2(t - \vartheta) - w_2], \\ \frac{d^p w_3(t)}{dt^p} = w_3 [g_2(w_1) - (a + \kappa_1 w_2(t - \vartheta) + \kappa_2 w_3(t - \vartheta))] \\ \quad + \tau_p [w_3 - w_{3*}] + \tau_d \frac{d^p [w_3 - w_{3*}]}{dt^p}, \end{array} \right. \quad (60)$$

where $p = 0.93$, $a = 1.4$, $\kappa_1 = 2.2$, $\kappa_2 = 1.05$, $w_0 = 1$, $\gamma_1 = 1$, $\gamma_2 = 1$, $g_1(w_1) = \frac{3w_1}{0.25+w_2}$, $g_2(w_1) = \frac{5w_1}{0.8+w_2}$. Let $\rho_1 = 0.2$, $\rho_2 = 0.5$, $\tau_p = 0.5$, $\tau_d = 0.4$. We can easily obtain that system (60) owns the unique positive equilibrium point $W(w_{1*}, w_{2*}, w_{3*}) = W(0.5750, 0.2127, 0.2123)$. The three assumptions (Q_1) , (Q_4) , (Q_5) of Theorem 4.1 are fulfilled. With the aid of Matlab software, one can get $\epsilon_0 = 2.8963$, $\vartheta_* = 2.32$. To check the correctness of the main conclusions of Theorem 4.1, we take two delays as examples. Firstly, select $\vartheta = 2.15$ which means $\vartheta < \vartheta_* = 2.32$, that is to say, ϑ falls into the range $[0, \vartheta_*)$. To this case, the Matlab simulation figures are displayed in Figure 6. Obviously, figure 6 manifests that the limiting nutrient concentration w_1 will be closed to 0.5750, the concentration of the first competitor w_2 will be closed to 0.2127 and the concentration of the second competitor w_3 will be closed to 0.2123 as $t \rightarrow +\infty$. Secondly, choose $\vartheta = 2.53$ which means $\vartheta > \vartheta_* = 1.91$, that is to say, ϑ exceeds the threshold delay number ϑ_* . To this case, the Matlab simulation figures are displayed in Figure 7. Obviously, Figure 7 manifests that the limiting nutrient con-

centration w_1 is about to remain a periodic oscillation state around 0.5750, the concentration of the first competitor w_2 is about to remain a periodic oscillation state around 0.2127 and the concentration of the second competitor w_3 is about to remain a periodic oscillation state around 0.2123. That is to say, system (60) are to produce a limit cycle (namely, Hopf bifurcation) near $W(w_{1*}, w_{2*}, w_{3*}) = W(0.5750, 0.2127, 0.2123)$. Furthermore, the bifurcation figures of system (60) are provided to embody the bifurcation point $\vartheta_* = 2.32$ (see Figures 8-10).

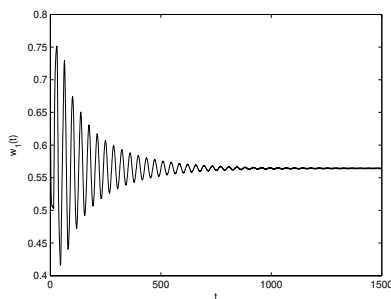


Figure 1. Computer experiment figures of system (59) with the time delay $\vartheta = 1.82 < \vartheta_0 = 1.91$. The positive equilibrium point $W(w_{1*}, w_{2*}, w_{3*}) = W(0.5750, 0.2127, 0.2123)$ maintains locally asymptotically stability. Horizontal axis represents t and longitudinal axis represents $w_1(t)$.

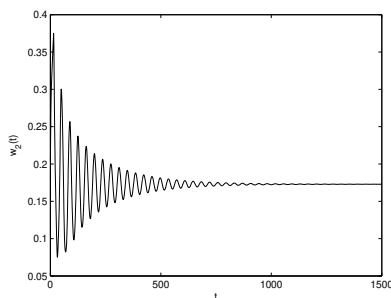


Figure 2. Computer experiment figures of system (59) with the time delay $\vartheta = 1.82 < \vartheta_0 = 1.91$. The positive equilibrium point $W(w_{1*}, w_{2*}, w_{3*}) = W(0.5750, 0.2127, 0.2123)$ maintains locally asymptotically stability. Horizontal axis represents t and longitudinal axis represents $w_2(t)$.

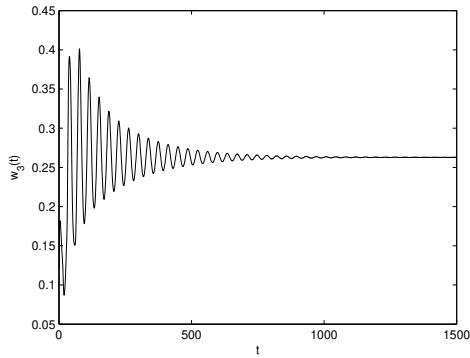


Figure 3. Computer experiment figures of system (59) with the time delay $\vartheta = 1.82 < \vartheta_0 = 1.91$. The positive equilibrium point $W(w_{1*}, w_{2*}, w_{3*}) = W(0.5750, 0.2127, 0.2123)$ maintains locally asymptotically stability. Horizontal axis represents t and longitudinal axis represents $w_3(t)$.

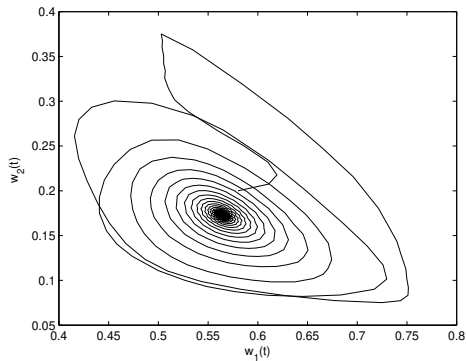


Figure 4. Computer experiment figures of system (59) with the time delay $\vartheta = 1.82 < \vartheta_0 = 1.91$. The positive equilibrium point $W(w_{1*}, w_{2*}, w_{3*}) = W(0.5750, 0.2127, 0.2123)$ maintains locally asymptotically stability. Horizontal axis represents $w_1(t)$ and longitudinal axis represents $w_2(t)$.

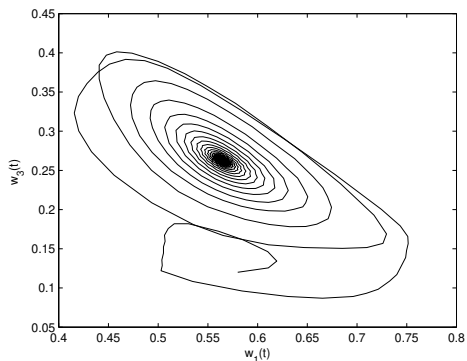


Figure 5. Computer experiment figures of system (59) with the time delay $\vartheta = 1.82 < \vartheta_0 = 1.91$. The positive equilibrium point $W(w_{1*}, w_{2*}, w_{3*}) = W(0.5750, 0.2127, 0.2123)$ maintains locally asymptotically stability. Horizontal axis represents $w_1(t)$ and longitudinal axis represents $w_3(t)$.

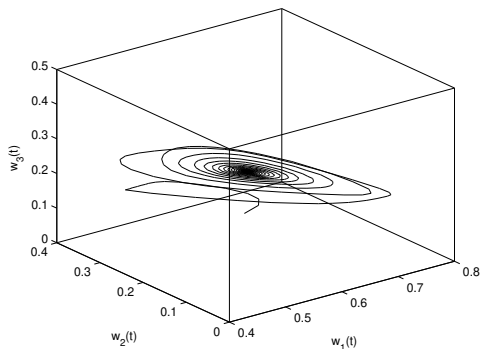


Figure 6. Computer experiment figures of system (59) with the time delay $\vartheta = 1.82 < \vartheta_0 = 1.91$. The positive equilibrium point $W(w_{1*}, w_{2*}, w_{3*}) = W(0.5750, 0.2127, 0.2123)$ maintains locally asymptotically stability. Horizontal axis represents $w_1(t)$, longitudinal axis represents $w_2(t)$ and vertical axis represents $w_3(t)$.

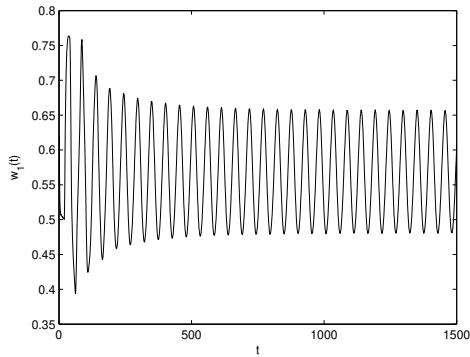


Figure 7. Computer experiment figures of system (59) with the time delay $\vartheta = 2.13 > \vartheta_0 = 1.91$. A limit cycle (Hopf bifurcation) happens near the positive equilibrium point $W(w_{1*}, w_{2*}, w_{3*}) = W(0.5750, 0.2127, 0.2123)$. Horizontal axis represents t and longitudinal axis represents $w_1(t)$.

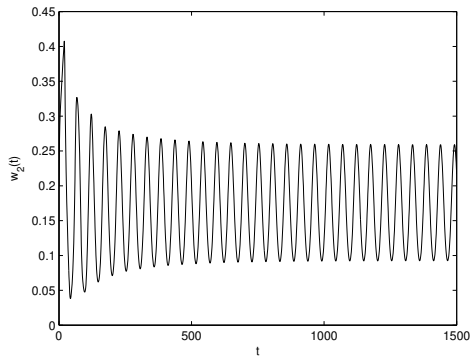


Figure 8. Computer experiment figures of system (59) with the time delay $\vartheta = 2.13 > \vartheta_0 = 1.91$. A limit cycle (Hopf bifurcation) happens near the positive equilibrium point $W(w_{1*}, w_{2*}, w_{3*}) = W(0.5750, 0.2127, 0.2123)$. Horizontal axis represents t and longitudinal axis represents $w_2(t)$.

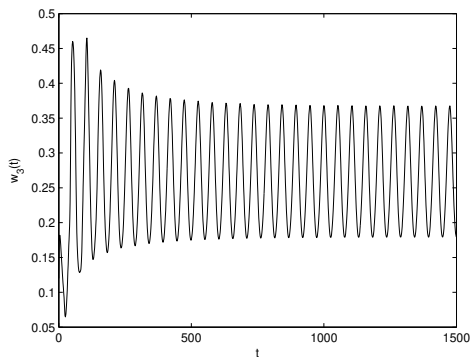


Figure 9. Computer experiment figures of system (59) with the time delay $\vartheta = 2.13 > \vartheta_0 = 1.91$. A limit cycle (Hopf bifurcation) happens near the positive equilibrium point $W(w_{1*}, w_{2*}, w_{3*}) = W(0.5750, 0.2127, 0.2123)$. Horizontal axis represents $w_1(t)$ and longitudinal axis represents $w_2(t)$.

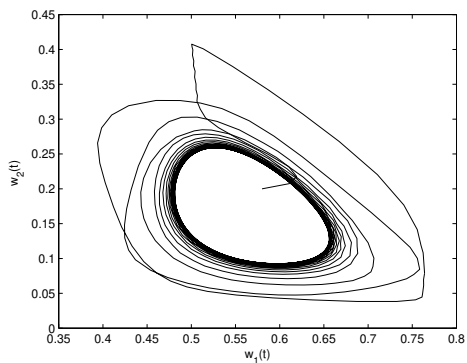


Figure 10. Computer experiment figures of system (59) with the time delay $\vartheta = 2.13 > \vartheta_0 = 1.91$. A limit cycle (Hopf bifurcation) happens near the positive equilibrium point $W(w_{1*}, w_{2*}, w_{3*}) = W(0.5750, 0.2127, 0.2123)$. Horizontal axis represents $w_1(t)$ and longitudinal axis represents $w_2(t)$.

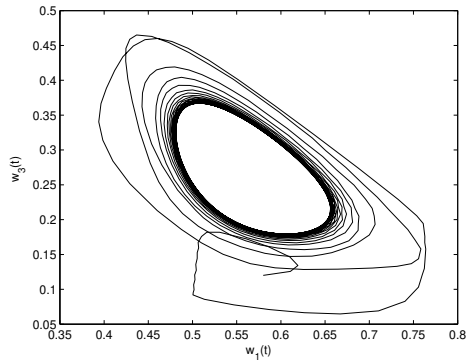


Figure 11. Computer experiment figures of system (59) with the time delay $\vartheta = 2.13 > \vartheta_0 = 1.91$. A limit cycle (Hopf bifurcation) happens near the positive equilibrium point $W(w_{1*}, w_{2*}, w_{3*}) = W(0.5750, 0.2127, 0.2123)$. Horizontal axis represents t and longitudinal axis represents $w_3(t)$.

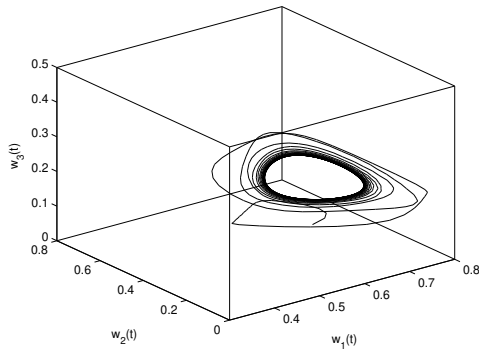


Figure 12. Computer experiment figures of system (59) with the time delay $\vartheta = 2.13 > \vartheta_0 = 1.91$. A limit cycle (Hopf bifurcation) happens near the positive equilibrium point $W(w_{1*}, w_{2*}, w_{3*}) = W(0.5750, 0.2127, 0.2123)$. Horizontal axis represents $w_1(t)$, longitudinal axis represents $w_2(t)$ and vertical axis represents $w_3(t)$.

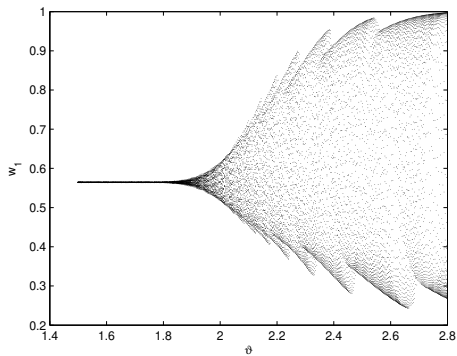


Figure 13. Bifurcation plot of system (59): the evolutionary relation of the time t and the variable w_1 . The bifurcation point of system (59) is 1.91.

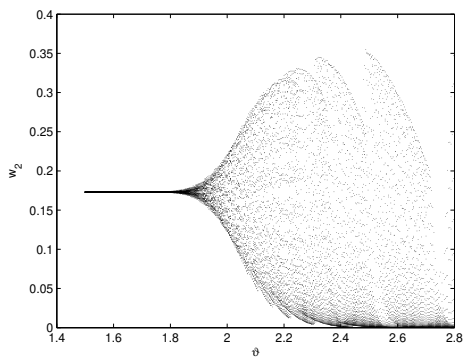


Figure 14. Bifurcation plot of system (59): the evolutionary relation of the time t and the variable w_2 . The bifurcation point of system (59) is 1.91.

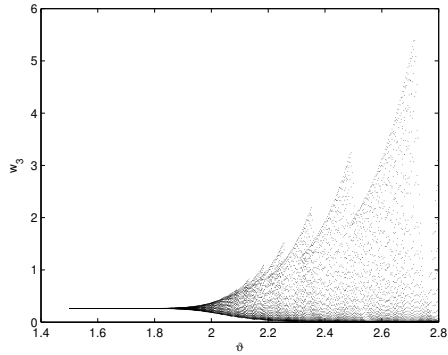


Figure 15. Bifurcation plot of system (59): the evolutionary relation of the time t and the variable w_3 . The bifurcation point of system (59) is 1.91.

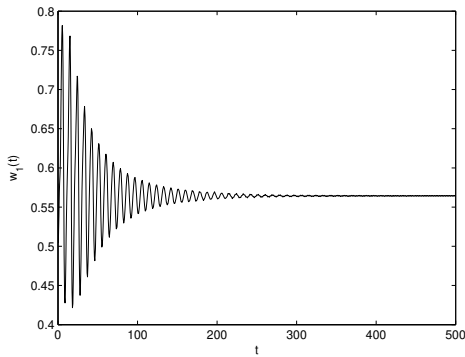


Figure 16. Computer experiment figures of system (60) with the time delay $\vartheta = 2.15 < \vartheta_* = 2.32$. The positive equilibrium point $W(w_{1*}, w_{2*}, w_{3*}) = W(0.5750, 0.2127, 0.2123)$ maintains locally asymptotically stability. Horizontal axis represents t and longitudinal axis represents $w_1(t)$.

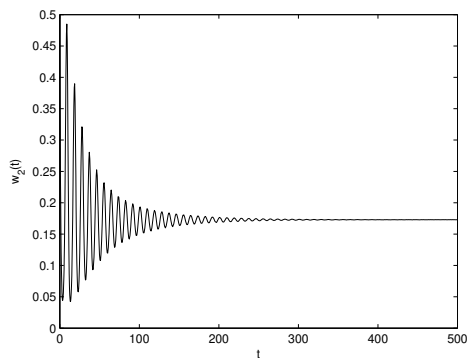


Figure 17. Computer experiment figures of system (60) with the time delay $\vartheta = 2.15 < \vartheta_* = 2.32$. The positive equilibrium point $W(w_{1*}, w_{2*}, w_{3*}) = W(0.5750, 0.2127, 0.2123)$ maintains locally asymptotically stability. Horizontal axis represents t and longitudinal axis represents $w_2(t)$.

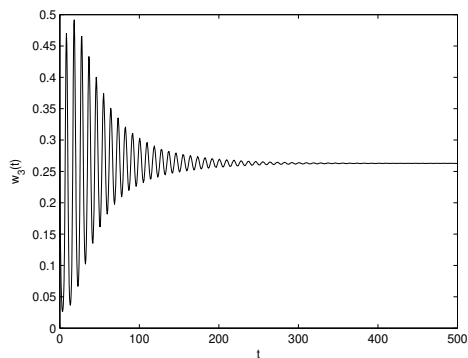


Figure 18. Computer experiment figures of system (60) with the time delay $\vartheta = 2.15 < \vartheta_* = 2.32$. The positive equilibrium point $W(w_{1*}, w_{2*}, w_{3*}) = W(0.5750, 0.2127, 0.2123)$ maintains locally asymptotically stability. Horizontal axis represents t and longitudinal axis represents $w_3(t)$.

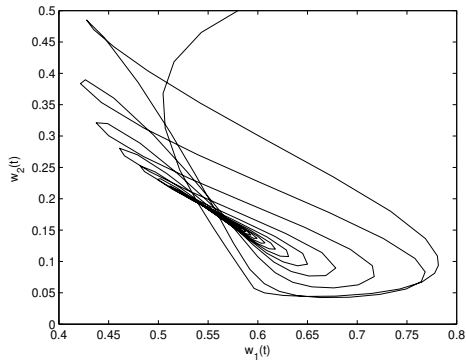


Figure 19. Computer experiment figures of system (60) with the time delay $\vartheta = 2.15 < \vartheta_* = 2.32$. The positive equilibrium point $W(w_{1*}, w_{2*}, w_{3*}) = W(0.5750, 0.2127, 0.2123)$ maintains locally asymptotically stability. Horizontal axis represents $w_1(t)$ and longitudinal axis represents $w_2(t)$.

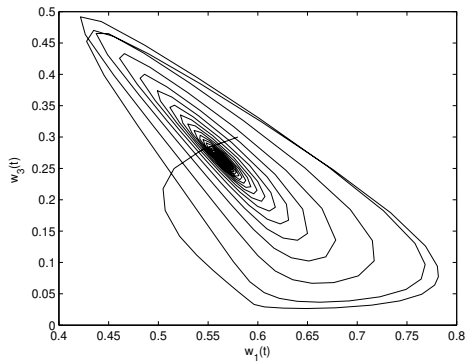


Figure 20. Computer experiment figures of system (60) with the time delay $\vartheta = 2.15 < \vartheta_* = 2.32$. The positive equilibrium point $W(w_{1*}, w_{2*}, w_{3*}) = W(0.5750, 0.2127, 0.2123)$ maintains locally asymptotically stability. Horizontal axis represents $w_1(t)$ and longitudinal axis represents $w_3(t)$.

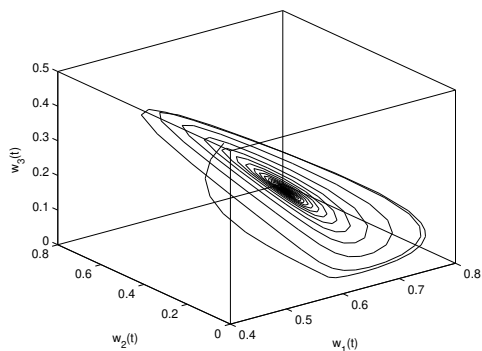


Figure 21. Computer experiment figures of system (60) with the time delay $\vartheta = 2.15 < \vartheta_* = 2.32$. The positive equilibrium point $W(w_{1*}, w_{2*}, w_{3*}) = W(0.5750, 0.2127, 0.2123)$ maintains locally asymptotically stability. Horizontal axis represents $w_1(t)$, longitudinal axis represents $w_2(t)$ and vertical axis represents $w_3(t)$.

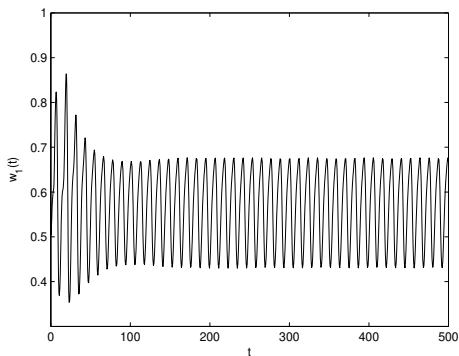


Figure 22. Computer experiment figures of system (60) with the time delay $\vartheta = 2.15 > \vartheta_* = 2.32$. A limit cycle (Hopf bifurcation) happens near the positive equilibrium point $W(w_{1*}, w_{2*}, w_{3*}) = W(0.5750, 0.2127, 0.2123)$. Horizontal axis represents t and longitudinal axis represents $w_1(t)$.

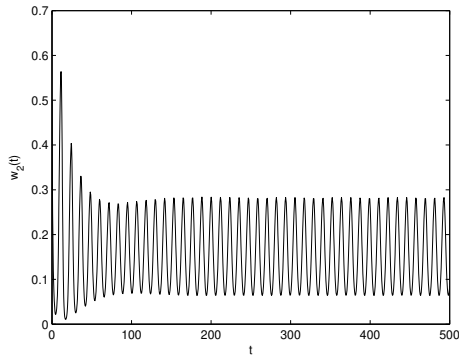


Figure 23. Computer experiment figures of system (60) with the time delay $\vartheta = 2.15 > \vartheta_* = 2.32$. A limit cycle (Hopf bifurcation) happens near the positive equilibrium point $W(w_{1*}, w_{2*}, w_{3*}) = W(0.5750, 0.2127, 0.2123)$. Horizontal axis represents t , longitudinal axis represents $w_2(t)$.

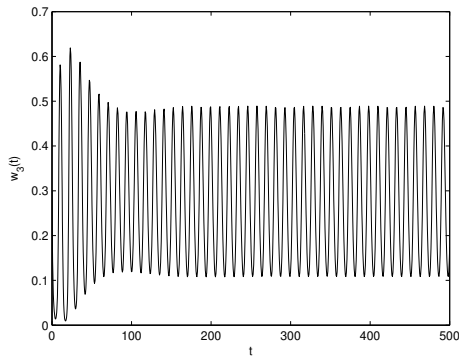


Figure 24. Computer experiment figures of system (60) with the time delay $\vartheta = 2.15 > \vartheta_* = 2.32$. A limit cycle (Hopf bifurcation) happens near the positive equilibrium point $W(w_{1*}, w_{2*}, w_{3*}) = W(0.5750, 0.2127, 0.2123)$. Horizontal axis represents t and longitudinal axis represents $w_3(t)$.

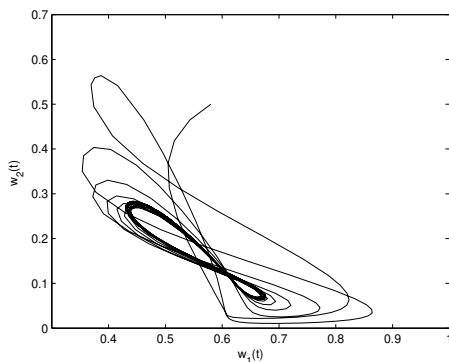


Figure 25. Computer experiment figures of system (60) with the time delay $\vartheta = 2.15 > \vartheta_* = 2.32$. A limit cycle (Hopf bifurcation) happens near the positive equilibrium point $W(w_{1*}, w_{2*}, w_{3*}) = W(0.5750, 0.2127, 0.2123)$. Horizontal axis represents $w_1(t)$ and longitudinal axis represents $w_2(t)$.

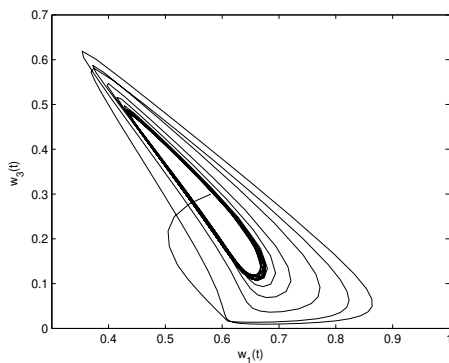


Figure 26. Computer experiment figures of system (60) with the time delay $\vartheta = 2.15 > \vartheta_* = 2.32$. A limit cycle (Hopf bifurcation) happens near the positive equilibrium point $W(w_{1*}, w_{2*}, w_{3*}) = W(0.5750, 0.2127, 0.2123)$. Horizontal axis represents $w_1(t)$ and longitudinal axis represents $w_3(t)$.

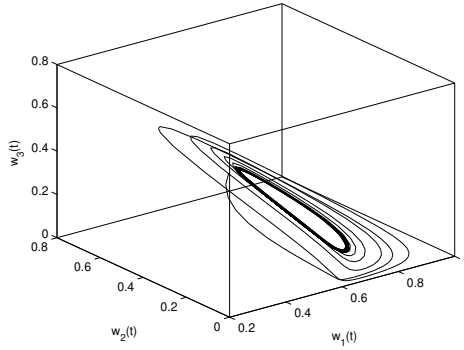


Figure 27. Computer experiment figures of system (60) with the time delay $\vartheta = 2.15 > \vartheta_* = 2.32$. A limit cycle (Hopf bifurcation) happens near the positive equilibrium point $W(w_{1*}, w_{2*}, w_{3*}) = W(0.5750, 0.2127, 0.2123)$. Horizontal axis represents $w_1(t)$, longitudinal axis represents $w_2(t)$ and vertical axis represents $w_3(t)$.

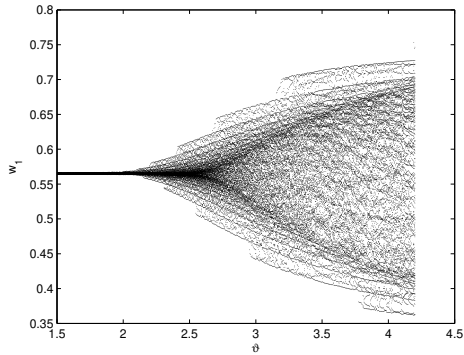


Figure 28. Bifurcation plot of system (60): the evolutionary relation of the time t and the variable w_1 . The bifurcation point of system (60) is 2.32.

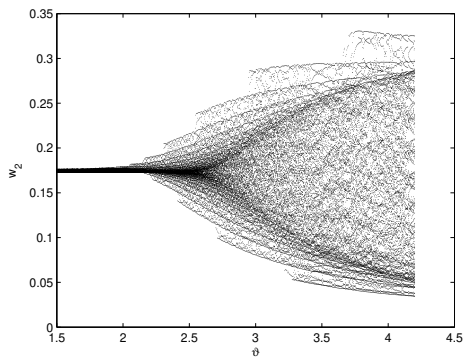


Figure 29. Bifurcation plot of system (60): the evolutionary relation of the time t and the variable w_2 . The bifurcation point of system (60) is 2.32.

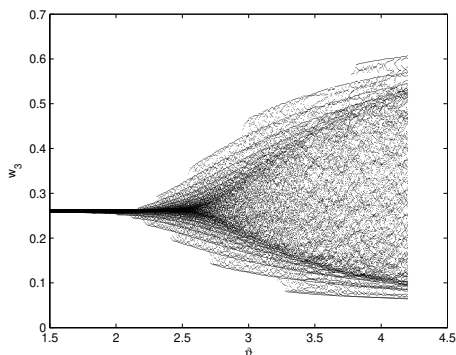


Figure 30. Bifurcation plot of system (60): the evolutionary relation of the time t and the variable w_3 . The bifurcation point of system (60) is 2.32.

Remark 5.1. From software simulation figures of Example 5.1 and Example 5.2, we can see that the bifurcation point of system (60) is 1.91 and the bifurcation point of system (60) is 2.32, which implies that the stability region of system (59) is enlarged and the time of onset of Hopf bifurcation of system (59) is postponed via the designed extended hybrid controller.

6 Conclusions

In recent year, in order to reveal the intrinsic evolution law of various chemical substances, many scholars have paid great attention to the exploration of differential chemical reaction models. Depending on the previous works, we set up a novel fractional-order delayed turbidostat model. Making use of laplace transform, stability and bifurcation knowledge of fractional-order dynamical system, we have investigated the stability and bifurcation behavior of the formulated fractional-order fractional-order delayed turbidostat model. A new sufficient criterion about bifurcation and stability of this model is gained. By virtue of extended hybrid controller, we have succeed in dominating the stability domain and the time of generation of Hopf bifurcation of the formulated fractional-order fractional-order delayed turbidostat model. In order to verify the validity of the acquired results, we give some Matlab simulations. The acquired outcomes have significant value in balancing and adjusting the concentrations of various chemical substances. The research methods are also exploited to handle many control problems in lots of differential dynamical systems. In addition, there are many works that focus on the stability and direction of Hopf bifurcation of inter-order delayed dynamical systems(see [52–54]), but we can deal with this topic due to the lack of basic theory for fractional-order dynamical equation.

Acknowledgment: This work is supported by National Natural Science Foundation of China (No.12261015, No.62062018), Project of High-level Innovative Talents of Guizhou Province ([2016]5651), Guizhou Key Laboratory of Big Data Statistical Analysis(No.[2019]5103), University Science and Technology Top Talents Project of Guizhou Province (KY[2018]047), Foundation of Science and Technology of Guizhou Province ([2019]1051), Guizhou University of Finance and Economics(2018XZD01).

References

- [1] C. J. Xu, Y. S. Wu, Bifurcation and control of chaos in a chemical system, *Appl. Math. Model.* **39** (2015) 2295–2310.

-
- [2] J. J. Wang, Y. F. Jia, Analysis on bifurcation and stability of a generalized Gray-Scott chemical reaction model, *Phys. A Stat. Mech. Appl.* **528** (2019) #121394.
- [3] C. H. Zhang, Y. He, Multiple stability switches and Hopf bifurcations induced by the delay in a Lengyel-Epstein chemical reaction system, *Appl. Math. Comput.* **378** (2020) #125201.
- [4] Z. Eskandari, R. K. Ghaziani, Z. Avazzadeh, B. Li, Codimension-2 bifurcations on the curve of the Neimark-Sacker bifurcation for a discrete-time chemical model, *J. Math. Chem.* (2023) doi: <https://doi.org/10.1007/s10910-023-01449-9>
- [5] A. Din, T. Donchev, D. Kolev, Stability, bifurcation and chaos control in chlorine dioxide-iodine-malonic acid reaction, *MATCH Commun. Math. Computer Chem.* **79** (2018) 577–606.
- [6] Y. Sekerci, S. Petrovskii, Mathematical modelling of plankton-oxygen dynamics under the climate change, *Bull. Math. Biol.* **77** (2015) 2325–2353.
- [7] T. K. Mankodi, U. V. Bhandarkar, B. P. Puranik, Hypersonic flow over Stardust Re-entry Capsule using abinitio based chemical reaction model, *Acta Astronautica* **162** (2019) 243–255.
- [8] D. Kim, M. S. Lee, S. B. Yun, On the positivity of an auxiliary function of the BGK model for slow chemical reactions, *Appl. Math. Lett.* **113** (2021) #106841.
- [9] S. Mondal, G. Samanta, Dynamics of a delayed toxin producing plankton model with variable search rate of zooplankton, *Math. Comput. Simul.* **196** (2022) 166–191.
- [10] A. Gökçe, S. Yazar, Y. Sekerci, Stability of spatial patterns in a diffusive oxygen-plankton model with time lag effect, *Math. Comput. Simul.* **194** (2022) 109–123.
- [11] V. Voorsluijs, Y.D. Decker, Emergence of chaos in a spatially confined reactive system, *Phys. D Nonlin. Phen.* **335** (2016) 1–9.
- [12] S. L. Yuan, P. Li, Y. L. Song, Delay induced oscillations in a turbidostat with feedback control, *J. Math. Chem.* **49** (2011) 1646–1666.
- [13] H. Smith, P. Waltman, *The Theory of the Chemostat*, Cambridge Univ. Press, Cambridge, 1995.

-
- [14] Z. Zhao, L. Yang, L. Chen, Impulsive state feedback control of the microorganism culture in a turbidostat, *J. Math. Chem.* **47** (2010) 1224–1239.
- [15] X. Meng, Z. Li, J. J. Nieto, Dynamic analysis of Michaelis-Menten chemostat-type competition models with time delay and pulse in a polluted environment, *J. Math. Chem.* **47** (2010) 123–144.
- [16] M. L. Shuler, F. Kargi, *Bioprocess Engineering Basic Concepts*, Prentice Hall, Englewood Cliffs, 1992.
- [17] N. S Panikov, *Microbial Growth Kinetics*, Chapman Hall, New York, 1995.
- [18] J. Flegr, Two distinct types of natural selection in turbidostat-like and chemostat-like ecosystems, *J. Theor. Biol.* **188** (1997) 121–126.
- [19] P. De Leenheer, H. L. Smith, Feedback control for the chemostat, *J. Math. Biol.* **46** (2003) 48–70.
- [20] C. J. Xu, D. Mu, Z. X. Liu, Y. C. Pang, M. X. Liao, C. Aouiti, New insight into bifurcation of fractional-order 4D neural networks incorporating two different time delays, *Commun. Nonlin. Sci. Numer. Simul.* **118** (2023) #107043.
- [21] C. J. Xu, Z. X. Liu, P. L. Li, J. L. Yan, L. Y. Yao, Bifurcation mechanism for fractional-order three-triangle multi-delayed neural networks, *Neural Process. Lett.* (2022) <https://doi.org/10.1007/s11063-022-11130-y>
- [22] C. J. Xu, W. Zhang, C. Aouiti, Z. X. Liu, L. Y. Yao, Bifurcation insight for a fractional-order stage-structured predator-prey system incorporating mixed time delays, *Math. Meth. Appl. Sci.* **46** (2023) 9103–9118.
- [23] C. J. Xu, D. Mu, Z. X. Liu, Y. C. Pang, M. X. Liao, P. L. Li, L. Y. Yao, Q. W. Qin, Comparative exploration on bifurcation behavior for integer-order and fractional-order delayed BAM neural networks, *Nonlin. Anal. Model. Control* **27** (2022) 1030–1053.
- [24] K. Udhayakumar, F. A. Rihan, R. Rakkiyappan, J. D. Cao, Fractional-order discontinuous systems with indefinite LKFs: An application to fractional-order neural networks with time delays, *Neural Netw.* **145** (2022) 319–330.

-
- [25] M. Xiao, W. X. Zheng, G.P. Jiang, Bifurcation and oscillatory dynamics of delayed cyclic gene networks including small RNAs, *IEEE Trans. Cyber.* **49** (2019) 883–896.
- [26] Y. T. Lin, J. L. Wang, C. G. Liu, Output synchronization analysis and PD control for coupled fractional-order neural networks with multiple weights, *Neurocomput.* **519** (2023) 17–25.
- [27] M. Xiao, W. X. Zheng, G. P. Jiang, J.D. Cao, Qualitative analysis and bifurcation in a neuron system with memristor characteristics and time delay, *IEEE Trans. Neural Netw. Learn. Syst.* **32** (2021) 1974–1988.
- [28] F. A. Rihan, C. Rajivganthi, Dynamics of fractional-order delay differential model of prey-predator system with Holling-type III and infection among predators, *Chaos Solit. Fract.* **141** (2020) #110365.
- [29] Z. Wang, Y. K. Xie, J. W. Lu, Y. X. Li, Stability and bifurcation of a delayed generalized fractional-order prey-predator model with interspecific competition, *Appl. Math. Comput.* **347** (2019) 360–369.
- [30] J. Xiao, L. Wu, A. L. Wu, Z.G. Zeng, Z. Zhang, Novel controller design for finite-time synchronization of fractional-order memristive neural networks, *Neurocomput.* **512** (2022) 494–502.
- [31] P. Liu, Y. L. Li, J. W. Sun, Y. F. Wang, Y. C. Wang, Event-triggered bipartite synchronization of coupled multi-order fractional neural networks, *Knowledge Based Syst.* **255** (2022) #109733.
- [32] C. J. Xu, D. Mu, Y. L. Pan, C. Aouiti, Y. C. Pang, L. Y. Yao, Probing into bifurcation for fractional-order BAM neural networks concerning multiple time delays, *J. Comput. Sci.* **62** (2022) #101701.
- [33] C. J. Xu, M. Farman, A. Akgül, K. S. Nisar, A. Ahmad, Modeling and analysis fractal order cancer model with effects of chemotherapy, *Chaos Solit. Fract.* **161** (2022) #112325.
- [34] C. J. Xu, M. Rahman, D. Baleanu, On fractional-order symmetric oscillator with offset-boosting control, *Nonlin. Anal. Modell. Control* **27** (2022) 994–1008.
- [35] F. F. Du, J. G. Lu, Adaptive finite-time synchronization of fractional-order delayed fuzzy cellular neural networks, *Fuzzy Sets Syst.* **466** (2023) #108480.

-
- [36] C. J. Xu, Z. X. Liu, Y. C. Pang, S. Saifullah, M. Inc, Oscillatory, crossover behavior and chaos analysis of HIV-1 infection model using piece-wise Atangana-Baleanu fractional operator: Real data approach, *Chaos Solit. Fract.* **164** (2022) #112662.
- [37] C. J. Xu, M. X. Liao, P. L. Li, L. Y. Yao, Q. W. Qin, Y. L. Shang, Chaos control for a fractional-order Jerk system via time delay feedback controller and mixed controller, *Fract. Fractional* **5** (2021) #257.
- [38] W. Ou, C. J. Xu, Q. Y. Cui, Z. X. Liu, Y. C. Pang, M. Farman, S. Ahmad, A. Zeb, Mathematical study on bifurcation dynamics and control mechanism of tri-neuron BAM neural networks including delay, *Math. Meth. Appl. Sci.* (2023) doi: <https://doi.org/10.1002/mma.9347>
- [39] C. J. Xu, Q.Y. Cui, Z. X. Liu, Y. L. Pan, X. H. Cui, W. Ou, M. Rahman, M. Farman, S. Ahmad, A. Zeb, Extended hybrid controller design of bifurcation in a delayed chemostat model, *MATCH Commun. Math. Comput. Chem.* **90** (2023) 609–648.
- [40] C. J. Xu, D. Mu, Y. L. Pan, C. Aouiti, L.Y. Yao, Exploring bifurcation in a fractional-order predator-prey system with mixed delays, *J. Appl. Anal. Comput.* **13** (2023) 1119–1136.
- [41] C. J. Xu, D. Mu, Z. X. Liu, Y. C. Pang, M. X. Liao, P.L. Li, Bifurcation dynamics and control mechanism of a fractional-order delayed Brusselator chemical reaction model, *MATCH Commun. Math. Comput. Chem.* **89** (2023)73–106.
- [42] C. J. Xu, X. H. Cui, P. L. Li, J. L. Yan, L. Y. Yao, Exploration on dynamics in a discrete predator-prey competitive model involving time delays and feedback controls, *J. Biol. Dyn.* **17** (2023) #2220349.
- [43] P. L. Li, Y. J. Lu, C. J. Xu,, J. Ren, Insight into Hopf bifurcation and control methods in fractional order BAM neural networks incorporating symmetric structure and delay, *Cogn. Comput.* (2023) doi: <https://doi.org/10.1007/s12559-023-10155-2>
- [44] D. Mu, C. J. Xu, Z. X. Liu, Y. C. Pang, Further insight into bifurcation and hybrid control tactics of a chlorine dioxide-iodine-malonic acid chemical reaction model incorporating delays, *MATCH Commun. Math. Comput. Chem.* **89** (2023) 529–566.
- [45] P. L. Li, R. Gao, C. J. Xu, J. W. Shen, S. Ahmad, Y. Li, Exploring the impact of delay on Hopf bifurcation of a type of BAM neural network models concerning three nonidentical delays, *Neural Process. Lett.* (2023) doi: <https://doi.org/10.1007/s11063-023-11392-0>

-
- [46] I. Podlubny, *Fractional Differential Equations*, Academic Press, New York, 1999.
- [47] D. Matignon, Stability results for fractional differential equations with applications to control processing, Computational engineering in systems and application multi-conference, *IEEE-SMC Proceed.* **2** (1996) 963–968.
- [48] H. L. Li, L. Zhang, C. Hu, Y. L. Jiang, Z. D. Teng, Dynamical analysis of a fractional-order predator-prey model incorporating a prey refuge, *J. Appl. Math. Comput.* **54** (2017) 435–449.
- [49] Z. Z. Zhang, H. Z. Yang, Hybrid control of Hopf bifurcation in a two prey one predator system with time delay, *Proceeding of the 33rd Chinese Control Conference*, Nanjing, China, 2014, pp. 6895–6900.
- [50] L. P. Zhang, H. N. Wang, M. Xu, Hybrid control of bifurcation in a predator-prey system with three delays, *Acta Phys. Sin.* **60**(2011) #010506.
- [51] L. Li, C. D. Huang, X. Y. Song, Bifurcation control of a fractional-order PD control strategy for a delayed fractional-order predator-prey system, *Eur. Phys. J. Plus* **138** (2023) #77.
- [52] M. X. Chen, R. C. Wu, X. H. Wang, Non-constant steady states and Hopf bifurcation of a species interaction model, *Commun. Nonlin. Sci. Numer. Simul.* **116** (2023) #106846.
- [53] D. D. Hassard, N. D. Kazarinoff, Y. H. Wan, *Theory and Applications of Hopf Bifurcation*, Cambridge Univ. Press, Cambridge, 1981.
- [54] M. X. Chen, Hopf bifurcation and self-organization pattern of a modified Brusselator model, *MATCH Commun. Math. Comput. Chem.* **90** (2023) 581–607.